Cement and Concrete Composites 142 (2023) 105201

Contents lists available at ScienceDirect

Cement and Concrete Composites

journal homepage: www.elsevier.com/locate/cemconcomp

The effect of oxygen and water on the provision of crack closure in bacteria-based self-healing cementitious composites

Linzhen Tan [a,c], Bianca Reeksting [b], Ismael Justo-Reinoso [c], Veronica Ferrandiz-Mas [c], Andrew Heath [c], Susanne Gebhard [b,d], Kevin Paine [c,*]

[a] School of Architecture, Building and Civil Engineering, Loughborough University, UK
[b] Life Sciences Department, Milner Centre for Evolution, University of Bath, UK
[c] Department of Architecture and Civil Engineering, University of Bath, UK
[d] Institut für Molekulare Physiologie, Mikrobiologie und Biotechnologie, Johannes Gutenberg-Universität Mainz, Germany

ARTICLE INFO

Keywords:
Crack
Water absorption
Healing regime
Oxygen releasing
Self-healing
Bacteria
MICP

ABSTRACT

This study determined the impact of oxygen and water on the crack healing performance of bacteria-based self-healing cementitious composites (BBSHCCs). Oxygen and water are considered essential to BBSHCCs using non-ureolytic bacteria, but in practice, the availability of either, for even short periods of time, cannot be guaranteed in the immediate aftermath of a crack forming. In this study, four healing regimes, (i) daily wet-dry cycle, (ii) weekly wet-dry cycle, (iii) semi-submerged and (iv) a deposition medium, were utilised to compare the impact of oxygen and water on the performance of BBSHCCs. Furthermore, an oxygen-releasing coating (ORC) containing calcium peroxide was evaluated and used in this study to further understand the function of oxygen in bacteria-based self-healing. Results showed that bacteria-based self-healing was only effective in wet conditions that also permit oxygen to penetrate the crack. Where there was a possibility for the composite to dry, after cracking, despite being wet some of the time the self-healing was far less efficient. It was observed that an overdose of nutrients and calcium in the healing environment resulted in early rapid healing, followed at a later stage by the dissolution of the initially formed precipitates. Moreover, it was found that the ORC contributed significantly to the recovery of both crack width and water tightness of samples. These findings will aid the development of appropriate test standards for self-healing cementitious composites and for the design and implementation of such cementitious composites in practice.

1. Introduction

Concrete dominates the infrastructure materials market due to its great durability, low cost, and reliable strength. However, inevitably cracks will occur in concrete during its service life. These cracks provide a pathway for the entry of deleterious substances that cause damage to concrete structures, e.g. corrosion of reinforcing steel or chemical degradation of the concrete itself [1]. Consequently in the UK, as an example, 46.4% of its total infrastructure budget (£84bn) has been spent in the last decade only to repair and maintain current infrastructure, a large proportion of which is concrete structures [2]. The development of innovative concrete that can self-repair these cracks could lead to significant reductions in maintenance costs.

Self-healing in cementitious composites can be achieved through enhanced autogenous healing [3–5] or autonomous healing processes. For the latter, encapsulation has been the preferred strategy to safeguard different chemical healing agents such as cyanoacrylate [6–9], epoxy [10–12], sodium silicate [13,14], silicon [15–17] or alkali-silica solutions [18]). In this regard, bacterial spores have also been encapsulated using porous particles (e.g. expanded clays [11–13], expanded perlite [14–16], aerated concrete granules [17–20]), fibres [21], polymers [22,23] and powder-compressed particles [24,25] to trigger healing of concrete via microbially induced calcite precipitation (MICP). Bacteria-based self-healing cementitious composites (BBSHCCs) are a significant contemporary research field [19–28]. Based on the process that leads to biomineralisation, MICP can be categorised into two main

Abbreviations: BBSHCC, Bacteria-based self-healing cementitious composite; GM, Growth media; ORC, Oxygen releasing coating; DIC, Dissolved inorganic carbon; MICP, Microbially induced calcite precipitation; R_W, Crack-width healing; R_P, Water-flow healing.

* Corresponding author. Centre for Climate Adaptation and Environment Research, University of Bath, BA2 7AY, UK.
E-mail address: k.paine@bath.ac.uk (K. Paine).

https://doi.org/10.1016/j.cemconcomp.2023.105201
Received 20 February 2023; Received in revised form 30 June 2023; Accepted 1 July 2023
Available online 7 July 2023

pathways: ureolytic and non-ureolytic. In the ureolytic pathway, MICP is achieved by the enzymatic hydrolysis of urea by the bacteria [29–34]. Despite the simplicity of the mechanism, a disadvantage to this pathway is that the by-production of ammonium from the hydrolysis of urea may cause potential environmental issues [35–37] and corrosion of reinforced steels [38–40]. In the non-ureolytic pathway, $CaCO_3$ is precipitated via bacterial degradation of organic compounds, such as calcium lactate [41] or calcium acetate [42], into calcium ions, dissolved inorganic carbon (DIC) and water; or alternatively by the dissolution of an inorganic salt (e.g., calcium nitrate) and the breakdown of a carbon-rich nutrient (e.g., yeast extract), with the latter leading to the production of DIC [43]. The high pH environment within the cement matrix allows for the conversion of the DIC to CO_3^{2-}, which in the presence of Ca^{2+} from either an added calcium source or from the cement hydration products [44], is precipitated as $CaCO_3$ [26].

It is known that water and oxygen are essential components for the main MICP pathways (i.e., urea degradation and organic carbon oxidation) [21,24,45]. In this regard, once a crack is formed, oxygen is readily available for bacteria, while the permeated water dissolves growth media and creates an appropriate environment for bacteria to grow. Many studies have demonstrated the major influence oxygen has on MICP as it ensures bacterial growth and promotes spore germination [46–48]. However, Wang et al. [49] observed that oxygen is not strictly needed for the enzymatic decomposition of urea when using ureolytic bacteria. Nevertheless, it is known that a steady oxygen supply is needed to sustain the high bacterial metabolic activity and efficiently induce $CaCO_3$ precipitation. In this context, Palin et al. [27] observed that for aerobic non-ureolytic bacteria, more than 1.5 mmol/l of oxygen could be consumed over 14 days to produce ~1 mm^3 of calcite. On the other hand, water has a key impact not only on the survival of bacteria but also on crucial aspects of bacterial life, such as the exchange of genetic material, motility and communication [50,51]. Moreover, water can directly influence self-healing efficiency through its temperature and pressure gradient [26].

Efforts have been made to optimise the healing conditions for BBSHCCs during laboratory experiments, although in practice, environmental conditions are uncontrolled. In this context, practically all the BBSHCC studies conducted so far have investigated specimens that have been completely immersed in water during healing [40,52,53], placed in semi-submerged conditions [54] or investigated when exposed to 100% relative humidity (RH) conditions [55]. However, a few studies have focused on comparing the degree of healing that can take place for otherwise identical BBSHCC specimens in different environmental conditions [34,56–58]. In this regard, Wang and Snoeck [34] placed BBSHCCs containing microencapsulated ureolytic bacteria in four different healing conditions (>95% RH, immersion in water, immersion in deposition medium, and wet/dry cycles). They observed that wet-dry cycles significantly promoted healing while keeping the BBSHCCs at 95% RH produced no healing. Furthermore, Tziviloglou et al. [56] compared two healing scenarios (immersion in water and wet/dry cycles) using aerobic non-ureolytic bacteria. They noticed that BBSHCCs exposed to wet/dry cycles (12 h per cycle) presented significantly better crack healing than when continuously submerged in water. However, even though both studies investigated BBSHCCs, the differences in mix designs, constituent materials and the type of bacteria used do not allow for a valid comparison to fully understand the role oxygen and water play in the healing efficiency of BBSHCCs, particularly for BBSHCCs relying on aerobic non-ureolytic bacteria.

On the other hand, biochemical reactions during $CaCO_3$ precipitation also rely on oxygen availability. In this context, Zhang et al. [59,60] found that the use of oxygen-releasing tablets (ORTs) alongside bacteria resulted in four times more calcite precipitation than samples without ORTs. ORTs consisted of calcium peroxide (CaO_2) and lactic acid compressed together. The higher $CaCO_3$ precipitation observed was not only attributed to an extended bacterial metabolic activity but also to the reaction of CaO_2 with water leading to the formation of additional Ca^{2+}.

However, whilst the need for oxygen and water to achieve BBSHCCs using non-ureolytic bacteria is well recognised, there remains some uncertainty as to exactly how bacteria-based self-healing works in environments where oxygen and water are present, but potentially limited. In this study, for the first time, BBSHCCs using aerobic non-ureolytic bacteria were subjected to different healing regimes with varied wetting to drying phases.

Overall, four healing conditions were investigated in this study: (i) a daily wet-dry cycle healing regime (16 h wet/8 h dry), (ii) a weekly wet-dry cycle healing regime (3 days wet/4 days dry), (iii) a semi-submerged healing regime with sample constantly semi-submerged by water and semi-exposed to the atmosphere and (iv) a daily wet-dry cycle healing regime (16 h wet/8 h dry) where the water contained a deposition medium consisting of dissolved calcium (i.e., calcium nitrate or calcium acetate) and yeast extract. For all four healing conditions, a previously investigated BBSHCC known to self-heal in appropriate conditions was used [43]. In addition, an innovative BBSHCC, containing calcium peroxide (CaO_2) as an oxygen-releasing material to provide additional oxygen during healing was also used.

2. Materials

2.1. Bacterial strain

The alkaliphilic species *Bacillus cohnii* DSM 6307 was obtained from the German Collection of Microorganisms and Cell Cultures (DSMZ) (Braunschweig, Germany) and stored in 25% (v/v) glycerol at −80 °C. *B. cohnii* colonies were inoculated in lysogeny broth (LB) where the pH of the LB was adjusted to 9.5 using an alkaline solution (10% v/v) containing 100 ml/l sodium sesquicarbonate (42 g/l $NaHCO_3$ and 53 g/l Na_2CO_3 anhydrous). Bacterial spores were produced using a sporulation medium as described in Ref. [40] and collected by centrifugation (3800×*g*, 10 min) when the majority of the vegetative cells presented phase-bright spores when assessed using phase-contrast microscopy (48–72 h). Next, the spore pellets were washed thrice with chilled 10 mM Tris-HCl buffer (pH 9), followed by treatment with chlorhexidine digluconate (0.3 mg/ml, 30 min) to kill any remaining vegetative cells. Then, spore pellets were rewashed as described above and frozen at −80 °C followed by freeze-drying under vacuum overnight. Dilution plating (LB agar, pH 8.2) was used to determine the spore viability (colony forming unit (cfu)/g).

2.2. Growth media (GM)

Depending on the method for adding the growth media (GM), calcium acetate ($Ca(C_2H_3O_2)_2$, Sigma-Aldrich (UK)) or calcium nitrate tetrahydrate ($Ca(NO_3)_2{\cdot}4H_2O$, Sigma-Aldrich (UK)) were used at a concentration of 0.05 g/g cement. Yeast extract (Sigma-Aldrich (UK)) was used at a concentration of 0.01 g/g cement to supply nutrients for bacterial spore germination and growth. Where calcium acetate was used, it was encapsulated together with the yeast extract in aerated concrete granules (ACG), while when calcium nitrate was used, both it and the yeast extract were directly added to the mixing water. In both cases, the combination of calcium source and yeast extract is referred to as 'GM' in this study, whilst the combination of GM and bacteria are referred to as 'bio-agents'.

Calcium acetate was used for the encapsulated calcium source as it has been successfully used in this form in earlier research [55]. However, it cannot be used as a direct addition due to a known impact on the hydration of cement [42]. Consequently, calcium nitrate was used for direct addition as has been successfully demonstrated elsewhere [43].

2.3. Aerated concrete granules (ACG)

The ACG used in this study were a commercially available product supplied by Cellumat SA (Belgium). After sieving to obtain ACG particles

in the 1–4 mm size range, these particles were used in selected mixes to immobilise bacterial spores or as a carrier of calcium acetate and yeast extract. ACG particles had a water absorption capacity of 120% and a loose dry bulk density of 354 kg/m^3 [43].

2.4. Encapsulation and immobilisation process

ACG were used to (i) encapsulate GM (calcium acetate and yeast extract) or (ii) immobilise bacterial spores. The procedure for this was as fully described in Tan et al. [43], where a vacuum chamber was set up with two-entry valves, one connected to a reservoir with either GM or bacterial spores, and the other valve was connected to a vacuum channel at 0.8 bar. ACG particles were saturated to achieve maximum storage of GM or bacterial spores. The encapsulation/immobilisation process was done independently to produce either ACG particles containing GM or bacterial spores and referred to henceforth as ACGM and ACGS, respectively.

After encapsulation/immobilisation, the ACG particles were dried at 80 °C for 24 h and then coated. Two types of coatings were used in this study: (i) PVA (polyvinyl acetate) and (ii) ORC (oxygen-releasing coating), as described below.

2.5. Coating material

2.5.1. PVA coating

Dried ACGM and ACGS particles were evenly coated with PVA (Bostik Ltd (UK)) using a titanium stand mixer equipped with a K-Blade (Kenwood (UK)). Mixing of the ACG particles and PVA proceeded until the PVA was slightly dried on the surface. Following this, the PVA-coated ACG particles were placed in an environmental chamber at 50% relative humidity and 20 °C for 24 h to achieve a dry surface. PVA-coated ACGM and ACGS particles were then stored in polythene bags until required. The mass ratio of PVA to plain ACG was 1:1, and the concentration of bacterial spores was approximately 3.9 × 10^9 spores per gram of PVA-coated ACGS. Less than 6% of PVA-coated ACGS or ACGM particles passed through a 2 mm sieve compared to 35% of un-coated ACG particles.

2.5.2. Oxygen-releasing coating (ORC)

An oxygen-releasing coating (ORC) was only applied to ACGS (i.e., containing bacterial spores), to ensure the availability and accessibility of oxygen close to the location of the bacterial spores. The ORC contained an inner layer of calcium peroxide (CaO_2) (Sigma-Aldrich (UK) and PVA, and an outer insoluble layer formed using a water-resistant adhesive, as shown in Fig. 1. To produce the inner layer, CaO_2 was mixed with PVA at a mass ratio between PVA and CaO_2 of 1:0.5. First, surface-dried ACGS were mixed with calcium peroxide powder using a titanium stand mixer (Kenwood (UK)), followed by the addition of PVA and further mixing. The inner-coated ACGS was dried at 50% relative humidity and 20 °C for 24 h. The outer coating consisted of a water-resistant adhesive comprised of acetone and propane (3 M Company™ (UK)). Surface-dried inner-coated ACGS were placed on non-stick paper and manually sprayed with a water-resistant adhesive (0.38 g adhesive/g ACG) to form a thin outer layer. The ORC-ACGS were then dried at 50% relative humidity and 20 °C for 24 h and stored in polythene bags until required.

The mean diameter of one ACG particle was 2.5 mm, as per the density of ACG (0.354 g/ml); the mass of one ACG particle was 0.0029 g. The mass ratio of an ACG particle: PVA: CaO_2 was 1: 1: 0.5, based on the densities of PVA and CaO_2 of 1.19 g/cm^3 and 2.91 g/cm^3, respectively. The density of the water-resistant adhesive was considered as 0.726 g/ml [61]. Therefore, the thickness of the inner layer (i.e., PVA and CaO_2) and the outer insoluble layer (i.e., water-resistant adhesive) were calculated as 0.16 mm and 0.06 mm, respectively; resulting in a total ORC thickness of 0.22 mm.

To determine the ability of the ORC-ACGS to release oxygen, broken and intact ORC- ACGS were submerged under water for 800 h and the released oxygen was collected and measured by displacement of a water column, as shown in Fig. 2. The ORC-AGS particles were split into two even pieces by cutting them with a knife.

2.6. Preparation of mortar prisms

Mortars were produced using Portland limestone cement (CEM II/A-L 32.5R) and standard sand conforming to BS EN 197-1 and BS EN 196-1, respectively. All mixes were prepared with the amount of tap water required to achieve a water/cement ratio of 0.5. Mortar prisms with dimensions of 65 mm × 40 mm × 40 mm were cast in two layers: the bottom layer (20 mm deep) contained bio-agents, whereas the top layer (20 mm deep) was designed using a standard mortar (referred to as REF)

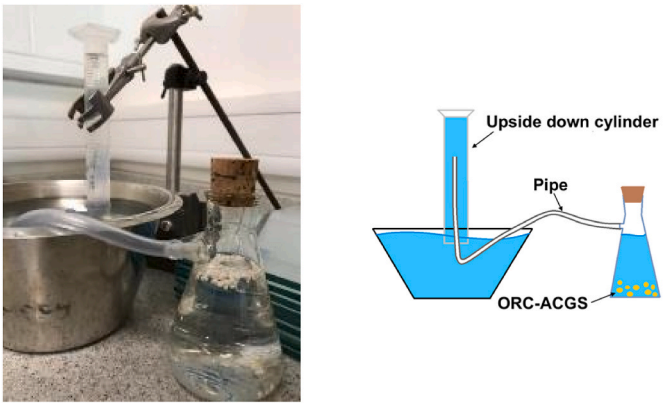

Fig. 2. Oxygen releasing test on ORC-ACGS, where ORC-ACGS were submerged in the flask with a pipe extended to an upside-down cylinder filled with water, and released oxygen was collected and measured as water displacement in the cylinder, (a) the apparatus and (b) the schematic image showing the set-up.

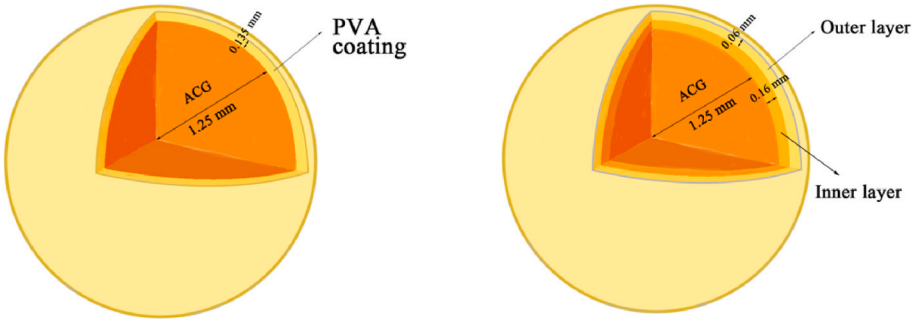

Fig. 1. Schematic image of PVA-ACGS (left) and ORC-ACGS (right).

for all samples. Three mortar prisms were cast for each mix.

The mix proportions of all bottom layers of the prisms are given in Table 1. CTRL represents the control sample with the direct addition of calcium nitrate and yeast extract. CN mortars contained ACGS and direct addition of calcium nitrate and yeast extract; CA contained ACGS and ACGM (encapsulated calcium acetate and yeast extract). CNO and CAO followed the same mixing proportions as CN and CA but using ORC-ACGS instead of PVA-coated ACGS. Mixing was carried out in accordance with BS EN 196-1, with the ACGM and ACGS (PVA-coated or ORC-coated) added at the same time as the sand. For the CTRL, CN and CNO specimens, the calcium nitrate and yeast extract were dissolved in the mixing water before they were added to the mixer. The bottom layer was cast approximately 1 h before the top layer. The specimens were wrapped in poly foil and cured at (20 °C, 40% RH) for 24 h. After demoulding, they were cured under water at 20 °C for 28 days.

2.7. Test methods

2.7.1. Hydration kinetics

Isothermal conduction calorimetry was carried out using an I-Cal 4000 (Calmetrix (USA)) to investigate the effect of the self-healing agents (calcium source, yeast extract, ORC and ACG) on the hydration of cement over the first 72 h. The intention of these tests was to determine whether there was any significant retardation that might results in different autogenous healing. , Tests were conducted at 20 °C on mortar samples. The mass of cement was fixed at 20 g in each mortar sample and other constituents were used at the same ratios as those for the main mortars as given in Table 1.

2.7.2. Crack creation

After curing, mortar prims were dried at 50 °C for 24 h to obtain a dry surface, and then the top 10–15 mm of all hardened prims were wrapped using a Tyfo® (FYFE (USA) carbon fibre-reinforced polymer (CFRP) composite system to prevent complete rupture of the prisms during cracking (Fig. 3). Prior to cracking, a notch of approximately 3 mm width and 1.5 mm depth was sawn at mid span to serve as the initiating point of cracking.

Prisms were subjected to three-point bending over a span of 60 mm, using a 30 kN Instron static testing frame (Fig. 3), with load applied at the centre point. The crack opening was measured with a crack mouth opening displacement (CMOD) transducer attached. The load was applied at a displacement rate of 0.2 mm/min and stopped when the crack was expected to be capable of elastically recovering to a width of 0.5 mm, i.e., they were initially cracked to around 0.8–1.0 mm in size depending on the ductility of the mortar. Three points of the crack per prism were stained with ink to facilitate the monitoring of crack closure over time with an optical microscope.

2.7.3. Healing regimes

Following cracking, mortar prisms were incubated for 84 days using one of the four healing regimes detailed below, with the schematic images of each regime given in Fig. 4. Specimens of all mortar mixes (i.e., REF, CTRL, CN, CNO, CA and CAO) were incubated using Methods A and B, while for Methods C and D, only specimens of REF, CTRL, CN and CA were incubated.

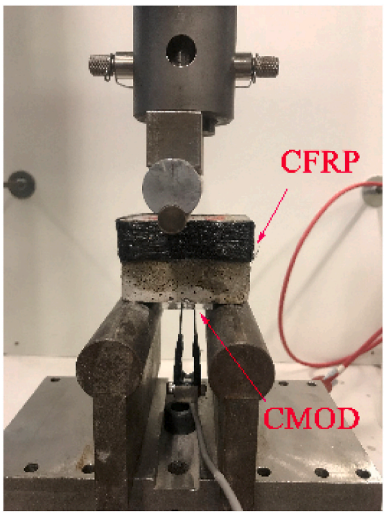

Fig. 3. Cracking generation via three-point bending with crack mouth opening displacement (CMOD) attached to monitor the crack width. CFRP was attached to prevent complete rupture.

2.7.3.1. Method A – Daily wet-dry cycle healing regime. For method A, as previously described by Tan et al. [43], samples were placed on a spacer of about 10 mm height in a plastic tank container, which was open to the atmosphere during the entire incubation period. A system to achieve a wet-dry cycle of 16-h wet and 8-h dry was created using automatically controlled pumps, supplying or removing water to or from the container. The containers were kept at laboratory room temperature (i.e., 20 °C ± 2 °C) and their incubation water changed every two weeks to prevent any oversaturation of calcium ions.

2.7.3.2. Method B – Weekly wet-dry cycle healing regime. Method B used a system to achieve a wet-dry cycle where samples were exposed alternatively to 3-days wet and 4-days dry conditions. For this, mortar prisms were removed or returned to the water at the relevant times. As in Method A, the containers were kept at laboratory room temperature and the incubation water changed every two weeks.

2.7.3.3. Method C – Semi-submerged healing regime. In method C, mortar prisms were kept semi-submerged in water with the top 20 mm of the mortar exposed to the atmosphere, as fully described by Reeksting et al. [54]. Water was frequently refilled to maintain the initial level throughout the incubation period. Similarly, to methods A and B, containers in method C were kept at laboratory room temperature and the incubation water changed every two weeks.

Table 1
Mix proportions for the bottom layer (cracked portion) of mortar samples. The top layer, in all cases, was equivalent to REF.

Mix	Cement (g)	Water (g)	Standard sand (g)	B.Spores ($\times 10^{10}$)	Yeast extract (g)	Calcium nitrate (g)	PVA-coated ACGS (g)	OCR-ACGS (g)	ACGM (g)
REF	92	46	276	–	–	–	–	–	–
CTRL	92	46	276	–	1.0	4.55	–	–	–
CN	92	46	260	3.64	1.0	4.55	3.5	–	–
CNO	92	46	260	3.64	1.0	4.55	–	4.4	–
CA	92	46	207	3.64	–	–	3.5	–	16.5[a]
CAO	92	46	207	3.64	–	–	–	4.4	16.5[a]

REF: standard mortar (plain mortar); CTRL: plain mortar without bacterial spores and growth media (GM) (i.e., calcium nitrate and yeast extract) directly added; CN: plain mortar with directly added GM and ACGS; CNO: plain mortar with directly added GM and ORC-ACGS; CA: plain mortar with the addition of ACGM (containing calcium acetate and yeast extract) and ACGS; and CAO: plain mortar with the addition of ACGM and ORC-ACGS.

[a] Including 1 g yeast extract and 4.55 g calcium acetate.

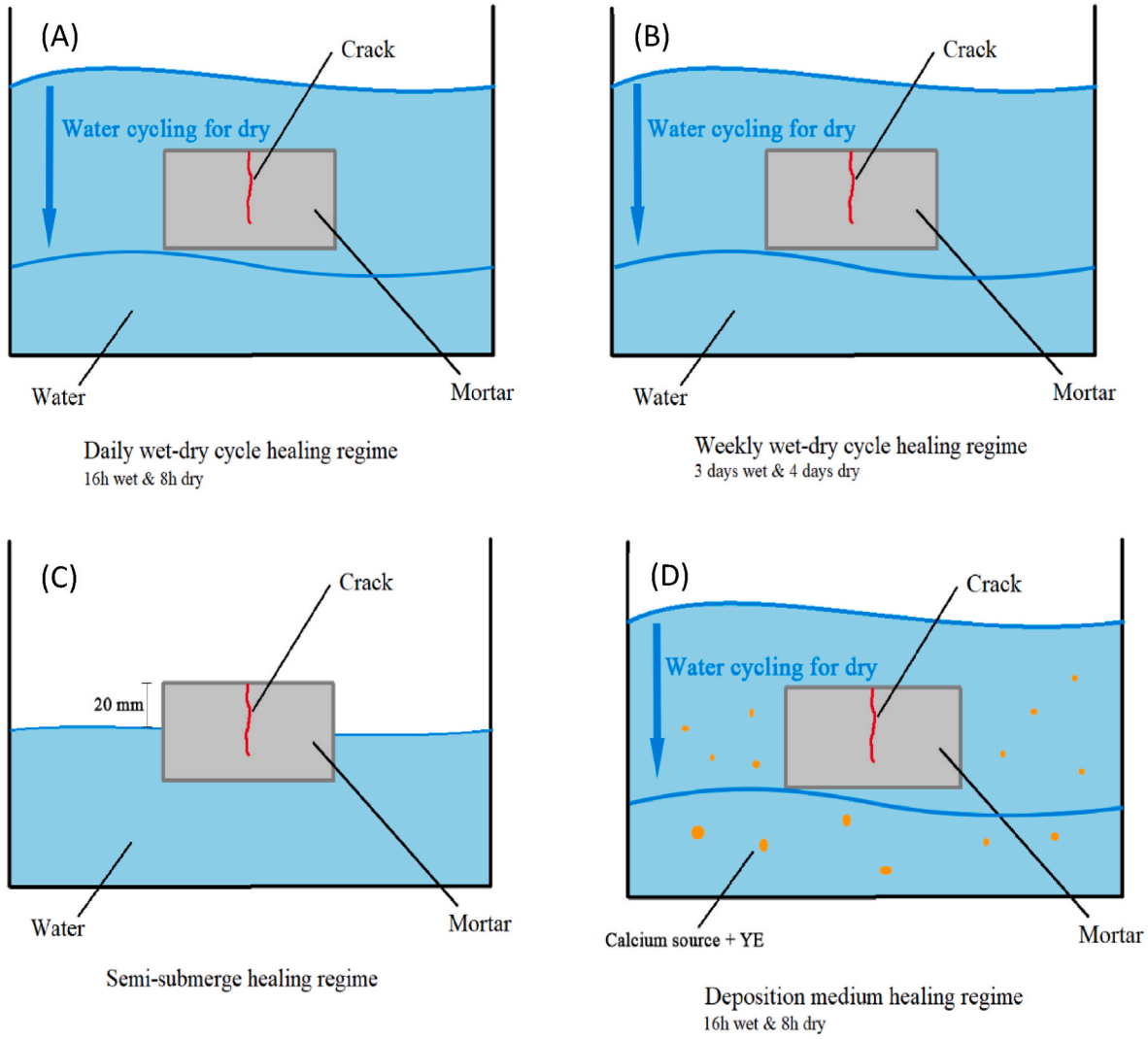

Fig. 4. Schematic set-up of four healing regimes, (a) daily wet-dry cycle healing regime, (b) weekly wet-dry cycle healing regime, (c) semi-submerged healing regime and (d) daily wet-dry cycle deposition medium healing regime. All mixes were subjected to healing regimes of (a) and (b), while REF, CTRL, CN and CA were placed in healing regimes of (c) and (d).

2.7.3.4. Method D – Daily wet-dry cycle deposition medium healing regime. In method D, a daily wet-dry cycle similar to the one used in method A was followed (i.e., 16-h wet and 8-h dry), with the difference that GM was dissolved in the incubation water to create a deposition medium healing regime to determine the potential limitation of GM for bacteria. The incubation medium was renewed every two weeks to maintain consistency. GM consisted of either calcium nitrate tetrahydrate or calcium acetate (10 g/l) and yeast extract (2 g/l), which were dissolved in the incubation water. REF, CTRL and CN mortar prisms were placed in the calcium nitrate-based deposition medium, while CA mortar prisms were placed in the calcium acetate-based deposition medium. Mortar prisms containing OCR-ACGS (i.e., CNO and CAO mixes) were not used in this healing regime.

2.8. Investigation of self-healing efficiency

2.8.1. Visualisation of crack-filling

A Leica M205C light microscope was used to visually observe the crack healing process. Images were taken on fresh cracks and then after 14, 28, 56 and 84 days of healing. The same ink-marked point was observed every time. The crack width healing percentage, *Rw (%)*, was determined by Equation (1):

$$R_W(\%) = \frac{W_0 - W_f}{W_0} \times 100\% \quad (1)$$

where W_0 was the initial crack width measured immediately after cracking, and W_f was the final crack width at 84 days.

2.8.2. Water-flow test

A water-flow test was carried out to investigate the progressive changes in migration of water due to crack healing. The same samples that were subjected to crack width measurement were also used for the water-flow tests. The water-flow test was a modified form of the RILEM Test Method 11.4 (Fig. 5) as previously described in Tan et al. [43], and the set-up of the apparatus is shown in Fig. 5(b). The water-flow coefficient, K, was obtained via Equation (2) (Cernica [62]).

$$K = \frac{aL}{At} ln\left[\frac{H_1}{H_2}\right] \quad (2)$$

where K = water-flow coefficient (cm/s); a = cross-sectional area of the pipette (cm^2), which was 1.33 cm^2. L = thickness of the specimen (cm); A = cross-sectional area of acrylic plate (cm^2), which was 15.27 cm^2; t = duration time of the test (s); H_1 = initial water head (cm), which was 12.4 cm; and H_2 = final water head (cm).

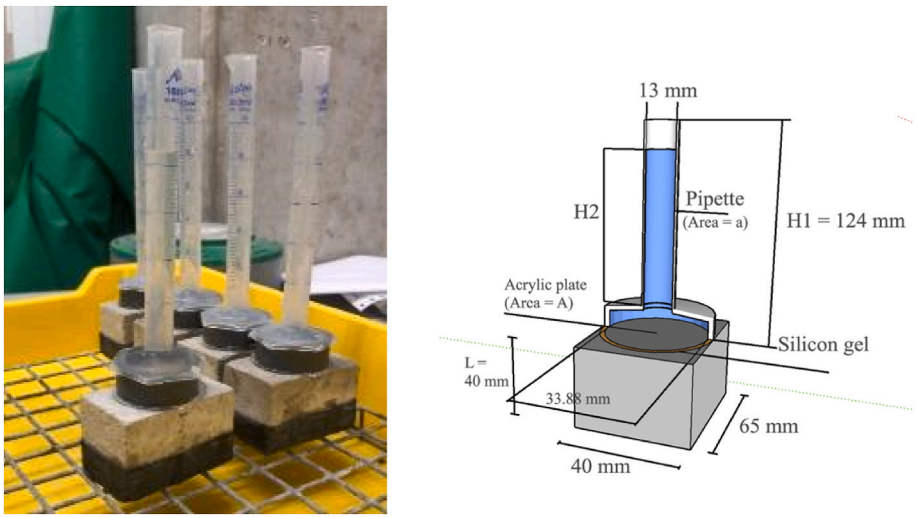

Fig. 5. Water-flow test apparatus (a) on site [43], (b) schematic.

The water-flow healing percentage, R_P *(%)*, was then calculated by Equation (3) where K_1 was the healed water-flow coefficient, and K_0 was the initial water-flow coefficient immediately after cracking.

$$R_P(\%) = \frac{K_0 - K_1}{K_0} \times 100\% \quad (3)$$

2.8.3. Scanning electron microscope (SEM) and energy dispersive X-ray (EDX) spectroscopy

Selected healed prisms were visualised under a scanning electron microscope (SEM) after 84 days of healing. Prior to SEM analysis, prisms were outgassed using an E306 Edward vacuum coating system for 72 h to remove any physically adsorbed water. Samples were examined at an accelerating voltage range of 10–15 kV using a JEOL JSM-6480LV SEM (Welwyn, UK) equipped with an energy-dispersive X-ray (EDX) analyser for elemental analysis. Backscattered electron (BSE) images were obtained in low vacuum without coating the samples. EDX, including line and mapping, was conducted in parallel to SEM to detect the elementary analysis of healing products. The different ACG particles used in this study (i.e., ACG, PVA-coated ACG and ORC-ACG) were analysed by SEM to identify the potential impact of coating on the morphology of these ACG particles. Prior to imaging, ACG particles were gold coated to avoid charging.

3. Results

3.1. Kinetics of hydration

Fig. 6 shows the relationship of hydration kinetics between each mortar mix over 72 h. Heat production rate and cumulative heat are presented as a ratio of the mass of cement. Generally, for mixes REF, CTRL, and CN, cement hydration kinetics followed the same behaviour as that observed by Tan et al. [43], where CTRL showed a retardation of cement hydration of about 20 h compared to REF – due to the presence of yeast extract, whereas CN showed 8 h retardation in this case with the yeast extract being compensated for by the presence of calcium nitrate.

In contrast, for CA and CAO, where growth media and bacterial spores were encapsulated, no significant hydration delay was noticed. CA and CAO generally showed a similar heat profile of hydration to REF, suggesting limited effect of adding encapsulated bio-agents on the cement hydration rate. Hence it can be concluded that the direct addition of yeast extract was the main reason causing the retardation [63]. Moreover, given the differences between CN and CA, ACG – as the carrier – was shown to efficiently prevent the leaking of GM during the mixing process. Furthermore, it should be noted that the utilisation of ORC, CAO and CNO to similar hydration rate and cumulative heat as CA and CN; suggesting that the outer coating (water-resistant adhesive) successfully isolated the inner layer containing calcium peroxide and the core containing the bio-agents from impacting on the cement hydration. However, the initial peak normally associated with C_3S hydration for the bio-mortars was lower than the REF mortar (2.9 mW/g). This is most

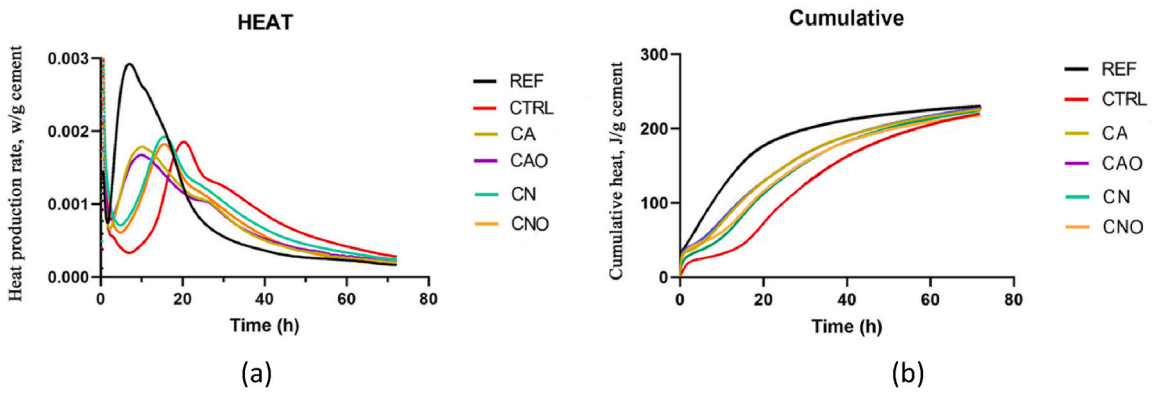

Fig. 6. Kinetics of hydration, (a) heat production rate, (b) cumulative heat.

likely due to differences in the thermal conductivity and specific heat capacity of sand and ACG particles. However, it is also noted that whilst the timing of the initial C_3S peak for CA and CAO generally occurred at the same time there were differences in the shape and timing of the secondary peak (normally associated with calcium aluminate hydration).

Overall the cumulative heat results, showed that all specimens produced similar heat at 72 h. This indicates that whilst the addition of ACG particles and GM may slow cement hydration, ultimately the degree of cement hydration would have been similar at the time of cracking (28 days) for all specimens. Therefore it is likely that by 28 days the cement in all specimens will have been effectively hydrated to the same degree. Consequently, any healing is not due to differences in autogenous healing and can be related to autonomic healing as provided by the self-healing materials used.

3.2. Properties of oxygen-releasing coating (ORC)

3.2.1. Oxygen releasing rate

To investigate the oxygen releasing efficiency of the ORC, both intact and broken pieces of ORC-ACGS were submerged in water to capture and quantify the amount of oxygen released, and the results converted to ml O_2/g ACG, as given in Fig. 7. For the broken ORC-ACGS, oxygen was released immediately upon their addition to water, and after 500 h, they had released 34 ml O_2/g ORC-ACGS. In contrast, for the intact ORC-ACGS, there was much less release of oxygen, as intended, although there was some leakage by 48 h, with more produced over the following 240 h. However, even after approximately 600 h, only 3.2 ml/g ORC-ACGS of oxygen was released. This suggests that the coating on the ORC-ACGS was sufficient to prevent the release of oxygen and that significant oxygen will only become available to the bacteria after the ORC-ACGS has been ruptured.

3.2.2. Morphology of the PVA and ORC

SEM was carried out to investigate the effect of coating on the morphology of the different ACG particles used in this study (i.e., plain ACG, PVA-coated ACG and ORC-ACG) (Fig. 8). Plain ACG had a coarse surface, while PVA-ACG was shown to be clearly covered by a film, most likely representing the PVA coating. A slightly more polished surface was observed in these PVA-coated ACG particles (Fig. 8(b)) that could suggest a likely lower adherence with the cementitious matrix, thus creating a weak plane that could lead to cracks not breaking these ACG particles rather than avoiding them. ORC-ACG presented a smooth surface attached by some powder, which was interpreted to be calcium peroxide. Nevertheless, considering the thickness of PVA and ORC was only calculated to be approximately 0.14 mm and 0.16 mm, respectively, both coatings were considered to have only minor impacts on the morphology of ACG particles. An indication on the thickness of each layer of coating is shown in the schematic image of Fig. 9. Further analysis of the effects that these different coatings might have on the physical or mechanical properties of cementitious materials was beyond the scope of this study.

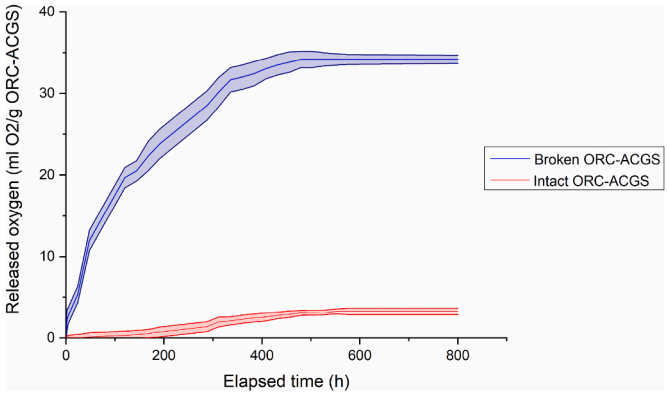

Fig. 7. The amount of released oxygen over 800 h by broken ORC-ACGS (blue) and intact ORC-ACGS (red). Note: the bands indicate the error bar. (For interpretation of the references to colour in this figure legend, the reader is referred to the Web version of this article.)

3.3. Healing

3.3.1. Visual observation of crack size

The crack width of each mortar was measured after cracking and then after 28, 56 and 84 days of healing. The mean crack width of the initial (W_0) and final cracks (W_1 at 84 days), along with the healing ratio (R_W), are given in Table 2. The healing evolution of each mortar mix is shown in Fig. 9.

In the daily wet-dry healing regime, CNO and CAO achieved the highest R_W of 100%, followed by CN and CA with about 98%; CTRL showed a R_W of 80%, whereas REF indicated no crack healing. In contrast, in the weekly wet-dry healing regime, it was noticeable that bacteria-based mortars demonstrated significantly reduced healing ratios compared to samples exposed to the daily wet-dry cycling, particularly for CAO, CA and CNO with R_W of 0%, 3% and 24%, respectively. Furthermore, in the semi-submerged healing regime, bacteria-based mortars (CA and CN) showed similar healing behaviour to those observed in the daily system. However, the R_W of the REF samples showed 47% healing without the addition of any bacteria or GM. Lastly, in the deposition medium healing regime, except for the REF samples that showed the highest R_W (50%), the overall healing capacity of the other mortars (CTRL, CN and CA) significantly declined when compared to equivalent samples exposed to the most similar healing regime (i.e., daily wet-dry healing regime).

In addition to crack-width measurement, the progress of crack closure was monitored visually during the healing period via an optical microscope. Figs. 10–13 show the initial (0 days) and final (84 days) crack appearance of a representative prism for each mortar mix incubated in the different healing regimes.

Clearly, the visual observation of mortars in the daily wet-dry cycle and semi-submerged healing regimes demonstrated overall greater healing than mortars in the other two systems after 84 days of incubation. For samples in the daily wet-dry system (Fig. 10), it was observed that no crystals were formed within the crack of REF samples over the entire healing period, while CTRL samples presented the opposite trend, where rapid healing occurred and the crack was blocked visually by 14 days. However, complete healing was not achieved by CTRL samples after 84 days. In contrast, bacteria-based specimens (i.e., CN, CA, CNO and CAO) showed greater healing, where CN and CA presented crystal formation on both faces of the cracks at 14 days, and complete crack closure appeared at 28 days. CNO and CAO presented the fastest healing with complete crack closure at 14 days.

On the other hand, when mortars were incubated in the weekly wet-dry cycle healing regime (Fig. 11), REF and CTRL samples performed similarly to that observed in the daily healing regime, where REF samples showed no crystals after 84 days and CTRL samples presented a rapid crystal formation at 28 days, but not complete healing after 84 days. However, bacteria-based mortars showed significantly less precipitation in the weekly regime than those in daily regime, with only a few precipitates observed at 84 days.

In the semi-submerged healing regime, healing was similar to that in the daily wet-dry cycle regime with the clear exception of REF (Fig. 12). Some progressive healing was observed for REF samples leading to Rw = 47%, rather than the zero-healing observed for equivalent REF samples incubated under a daily wet-dry cycle regime. It is possible that

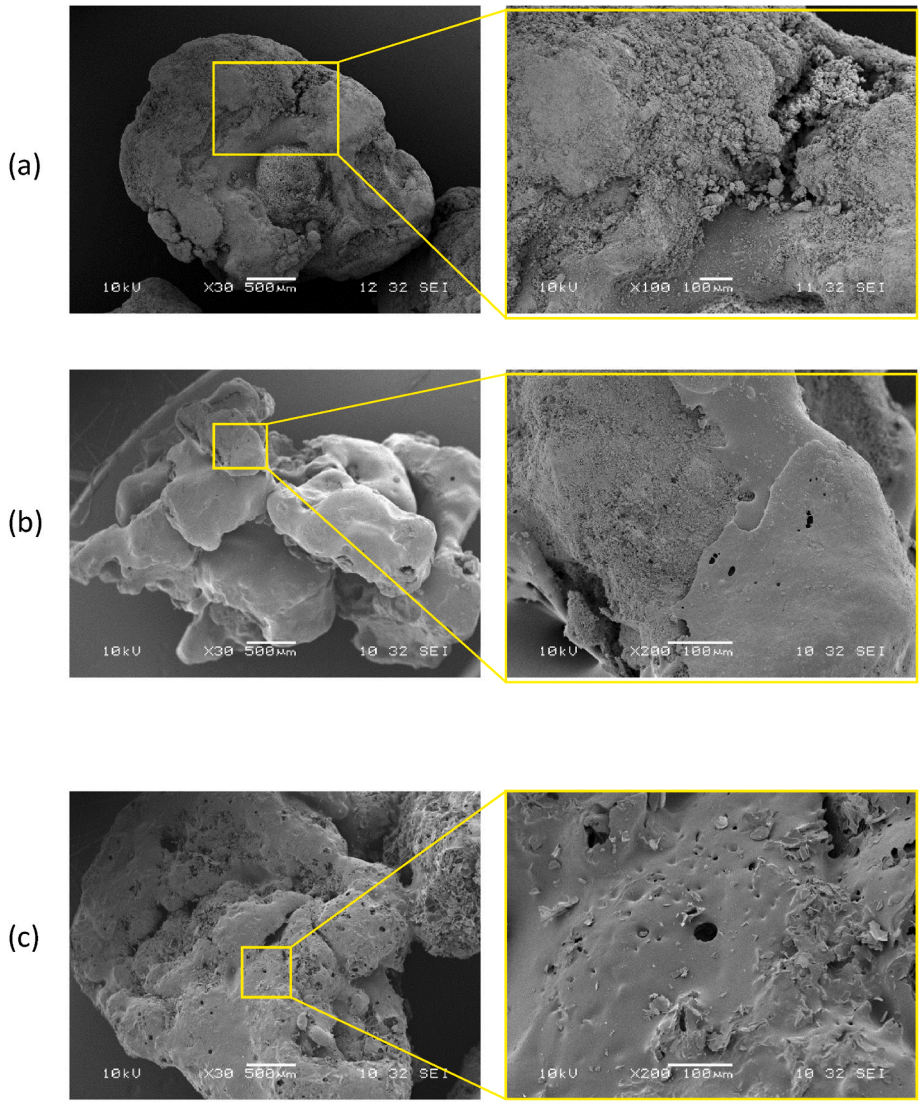

Fig. 8. Surface morphology of (a) plain ACG, (b) PVA-coated ACG and (c) ORC-ACG.

some leaching of calcium led to a build-up of calcium hydroxide and later calcium carbonate on the surface, which was not washed away by the water cycling as it is in the daily regime. With respect to the CTRL samples, large crystals were observed at 14 days and maximum healing occurred at 28 days with a crack closure of around 90%. CN samples had rapid healing precipitation with the crack completely healed at 28 days, similar to what was observed in the daily wet-dry cycle regime. Regarding CA samples, a slower precipitation rate was observed where only a few crystals were formed on the faces of crack after 14 days of incubation. Nevertheless, complete crack closure was observed at 84 days.

Cracks of mortars following the daily wet-dry cycle deposition medium healing regime are shown in Fig. 13. After 84 days in this healing regime, all samples had a large open crack with only a few precipitated crystals on the faces of these cracks. Progressive healing images of the cracks showed some large cubic crystals formed on REF and CTRL samples at 14 days; no further precipitation took place in the following days resulting in only slightly healed crack after 84 days of incubation. For CN and CA mortars, healing progressed well at the beginning where large crystals were extensively formed at 14 days and blocked the crack completely after 56 days of incubation. However, all of the precipitates formed disappeared after 84 days of incubation, leaving a reopened crack.

3.3.2. *Water-flow test results*

A water-flow test was conducted in parallel to the visual observations to evaluate the recovery of the water tightness of the mortar prisms as the crack healed (Table 3). Water-flow tests were conducted immediately after cracking (Day 0) and after 28, 56 and 84 days of healing. Intermediate measurements (between 0 and 28 days) were not conducted to avoid removal of newly formed precipitates as recommended by Roig-Flores et al. [64]. Fig. 14 shows the recovery of water flow resistance against time. In general, the water-flow healing (R_P) observed was consistent with the crack-width healing (R_W) described earlier. However, it is noted that whilst no crack healing was observed in the REF specimens there was a measurable recovery of permeability. This suggests that the two tests are not measuring exactly the same thing. The reduction in the permeability could be due to some autogenous healing deep within the crack where the crack width is much lower. Consequently, water flow would be reduced despite no apparent healing at the surface. Furthermore, the test does not directly measure flow through the crack alone, and the permeability of the uncracked mortar either side of the cracks possibly plays a role in the result generated. This uncracked mortar will be 84 days older, and less permeable, than when the test was initially carried out. So, it is possible that some of the reduction in permeability reflects the hardening of the mortar.

After being exposed for 84 days to the daily wet-dry cycle healing

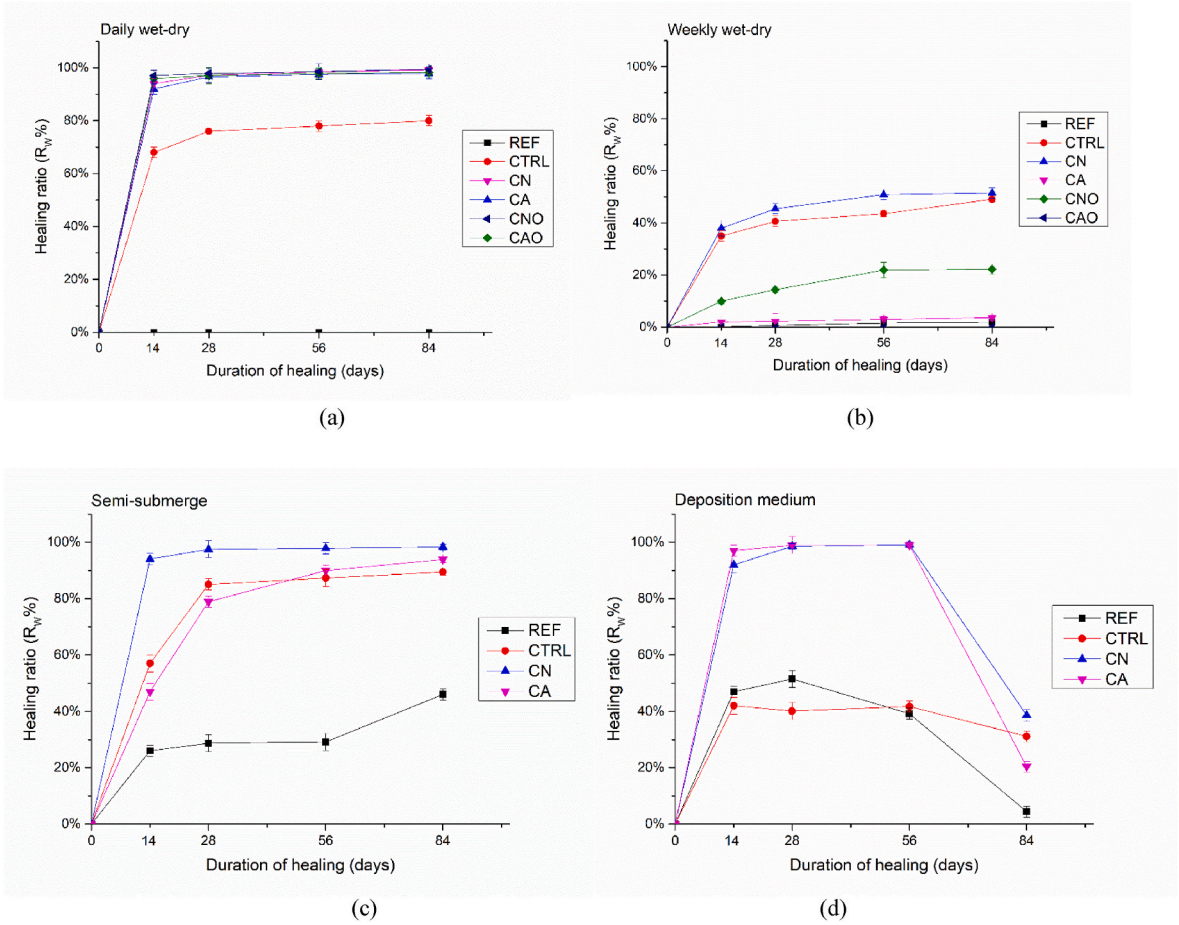

Fig. 9. Crack width progress over 84 days in the healing regimes of (a) daily wet-dry cycle, (b) weekly wet-dry cycle, (c) semi-submerged and (d) deposition medium.

regime, the R_P observed for REF was 35%, which was higher than the R_W (0%). The aforementioned result can likely be attributed to autogenous healing that occurred deeper in the crack and which it is not evident at the surface. Consistent with R_W results, in the daily wet-dry cycle healing regime, only CN showed a slightly lower R_P at 28 days than the other four mortars (CTRL, CA, CNO and CAO) (Fig. 14 (a)). Moreover, the R_P at 84 days for all mortars, except REF, were all around 100%, indicating the significant promoting effect of the daily wet-dry cycle healing regime on crack healing.

For the specimens exposed to the weekly wet-dry cycle healing regime, the final water-flow coefficients of all mortar prisms were significantly higher when compared to those observed for equivalent mortar prisms exposed to the daily wet-dry cycle regime. CTRL presented the highest R_P (72%) of all the mortars in the weekly condition, while the bacteria-based mortars revealed varying degrees of healing that could likely be considered low. Moreover, mortar samples containing ORC-ACG particles showed overall greater healing than mortar samples where PVA-coated ACG particles were used. The water-flow coefficient for REF fluctuated over the healing period (Fig. 14 (b)) and resulted in a generally unchanged K_1 at 84 days.

Semi-submerged healing regime results are shown in Fig. 14 (c). REF showed a significant higher R_P value (67%) when compared to equivalent REF mortars incubated in the two previous healing regimes, and where the most of the healing occurred in the first 56 days. The other three mortar mixes (CTRL, CA and CN) achieved high R_P values (99–100%), suggesting a high degree of healing.

For the specimens incubated in the daily wet-dry DM healing regime (Fig. 14 (d)), REF showed a gradually increased R_P value that resulted, after 84 days, in a very similar value as the one observed for the REF mortar incubated in a semi-submerged healing regime (66%). For CTRL, an early increase of R_P was detected over the first 56 days, but the ratio dropped slightly at 84 days and resulted in a final R_P of 66%. Furthermore, in agreement with the R_W values shown in Fig. 9 (d), CN and CA exhibited a rapid R_P rise at the beginning of the healing period, particularly at 28 days, but the R_P then dropped suddenly at 84 days leading to even lower R_P values than the ones observed for REF and CTRL.

3.3.3. *SEM and EDX of healing products*

An SEM-EDX line scan elemental analysis on a CN mortar sample after being exposed for 84 days to a daily wet-dry cycle healing regime is shown in Fig. 15. The SEM-EDX line scan shows the concentration of calcium, silicon, carbon and oxygen and was determined through the healing product on a side surface close to the top-notch. The elementary map showed that whilst the silicon concentration was generally low along the entire line, it was noticeably lower in the healing product compared to the mortar matrix. In contrast, the calcium concentration was shown to have an inverse trend presenting a higher concentration in the healing product than in the mortar matrix. It is noticeable that the calcium concentration near the edges of the original crack was also found to be relatively high, most likely due to the leaching of calcium ions from inside the mortar matrix to the vicinity of the crack and their consequent transformation into calcium carbonate when exposed to atmospheric CO_2.

The BSE and elementary maps (carbon, oxygen, silicon and calcium) of healed cracks on CN and CNO mortars exposed for 84 days to a daily wet-dry cycle healing regime are shown in Figs. 16 and 17, respectively. It should be noted that CNO demonstrated lower carbon but higher calcium concentration in the crack area than in the mortar matrix itself, while CN did not show this pattern. The introduction of ORC-ACGS in CNO may have resulted in an additional calcium hydroxide source due

Table 2
Mean value ± the standard deviation of the initial crack width (0 days), final crack width (84 days) and healing ratios percentages (R_W%) of prisms incubated in the four healing regimes.

	A. Daily wet-dry cycle			B. Weekly wet-dry cycle		
	Initial crack (mm)	Final crack (mm)	Healing ratio (R_W%)	Initial crack (mm)	Final crack (mm)	Healing ratio (R_W%)
REF	0.38 ± 0.03	0.38 ± 0.03	0% ± 0%	0.41 ± 0.03	0.40 ± 0.02	2% ± 0.3%
CTRL	0.21 ± 0.03	0.04 + 0.01	80% ± 2%	0.25 ± 0.03	0.12 ± 0.01	52% ± 1%
CN	0.43 ± 0.02	0.01 ± 0.00	98% ± 1%	0.38 ± 0.02	0.19 ± 0.01	50% ± 2%
CA	0.39 ± 0.04	0.01 ± 0.00	98% ± 2%	0.32 ± 0.03	0.31 ± 0.02	3% ± 1%
CNO	0.37 ±0.04	0.00 ± 0.00	100% ± 0%	0.37 ± 0.02	0.28 ± 0.02	24% ± 2%
CAO	0.35 ± 0.03	0.00 ± 0.00	100% ± 0%	0.28 ± 0.03	0.28 ± 0.03	0% ± 0%
	C. Semi-submerged			**D. Deposition medium**		
	Initial crack (mm)	Final crack (mm)	Healing ratio (R_W%)	Initial crack (mm)	Final crack (mm)	Healing ratio (R_W%)
REF	0.38 ± 0.02	0.20 ± 0.01	47% ± 2%	0.40 ± 0.03	0.38 ± 0.01	5% ± 2%
CTRL	0.38 ± 0.03	0.04 ± 0.01	90% ± 1%	0.37 ± 0.03	0.25 ± 0.02	32% ± 2%
CN	0.42 ± 0.03	0.01 ± 0.00	98% ± 1%	0.46 ± 0.04	0.28 ± 0.01	40% ± 2%
CA	0.41 ± 0.02	0.02 ± 0.01	94% ± 1%	0.38 ± 0.02	0.30 ± 0.01	21% ± 2%

Note: Shaded boxes represent samples taken for analysis under EDX and SEM.

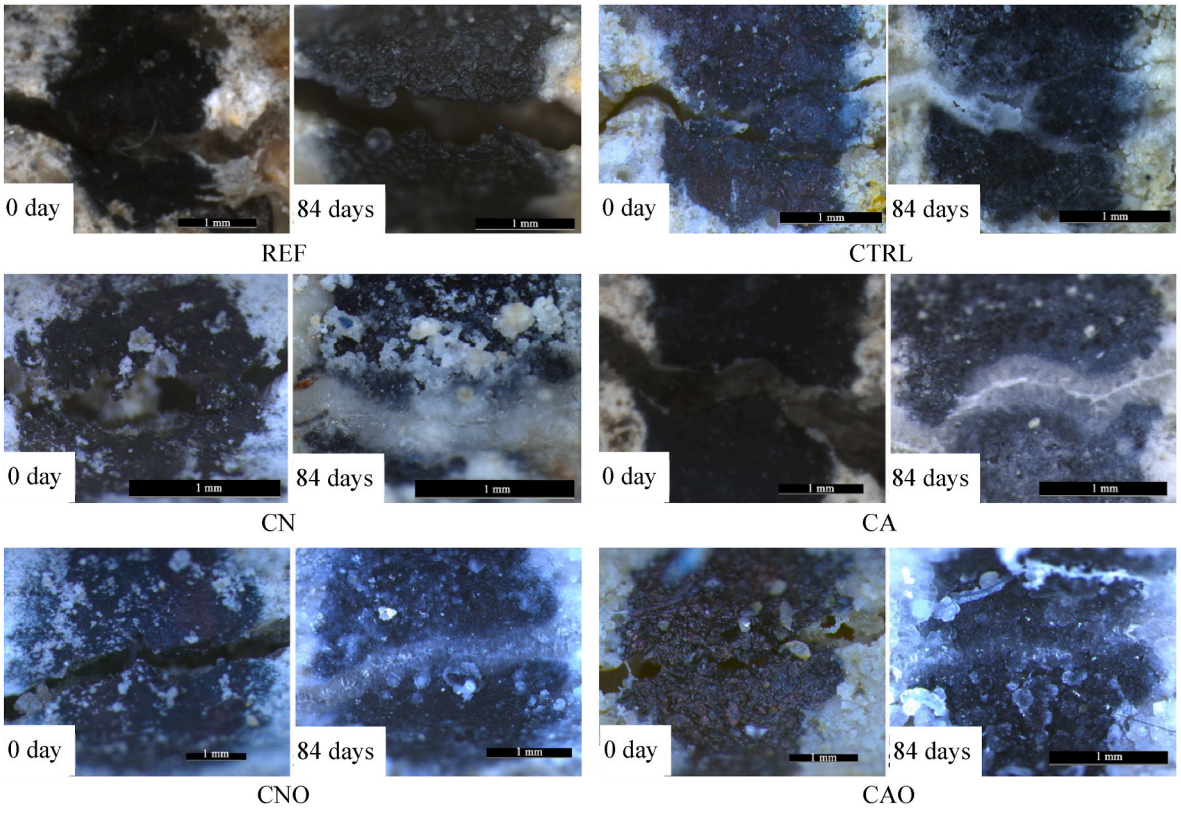

Fig. 10. Progression of crack healing of specimens in daily wet-dry cycle healing regime.

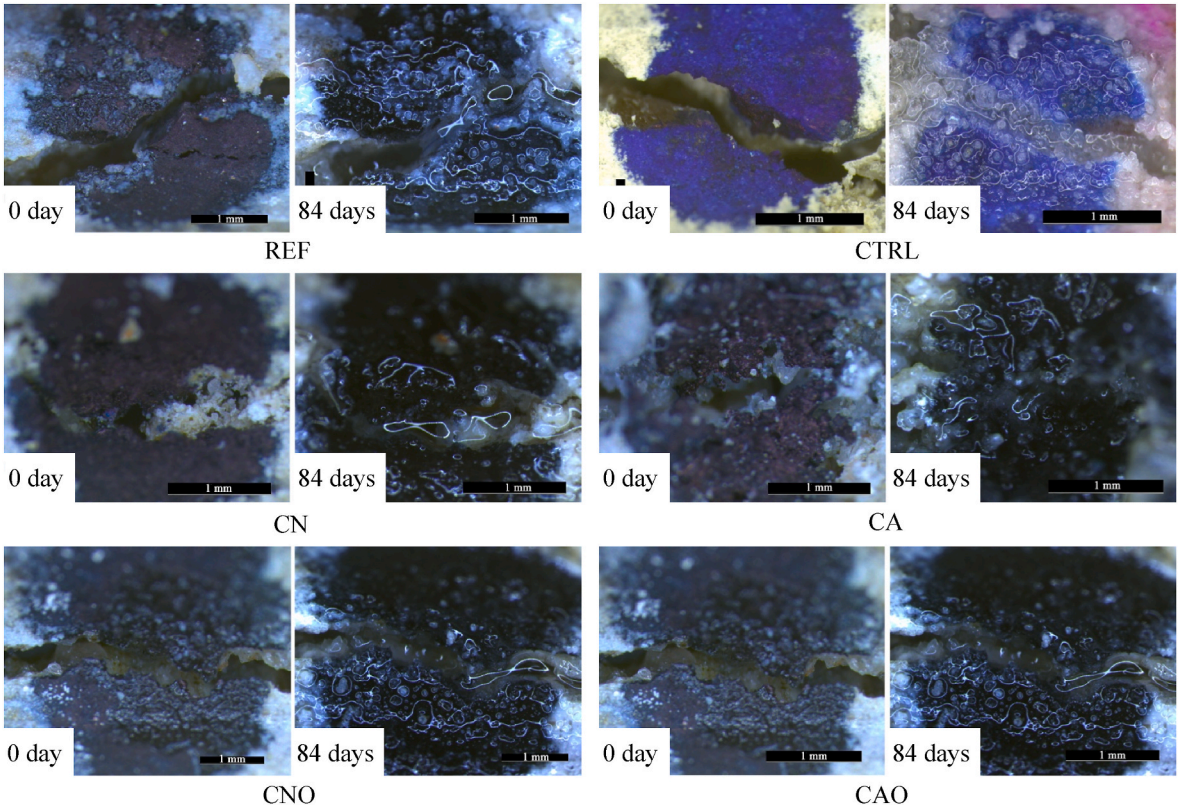

Fig. 11. Progression of crack healing of specimens in weekly wet-dry cycle healing regime.

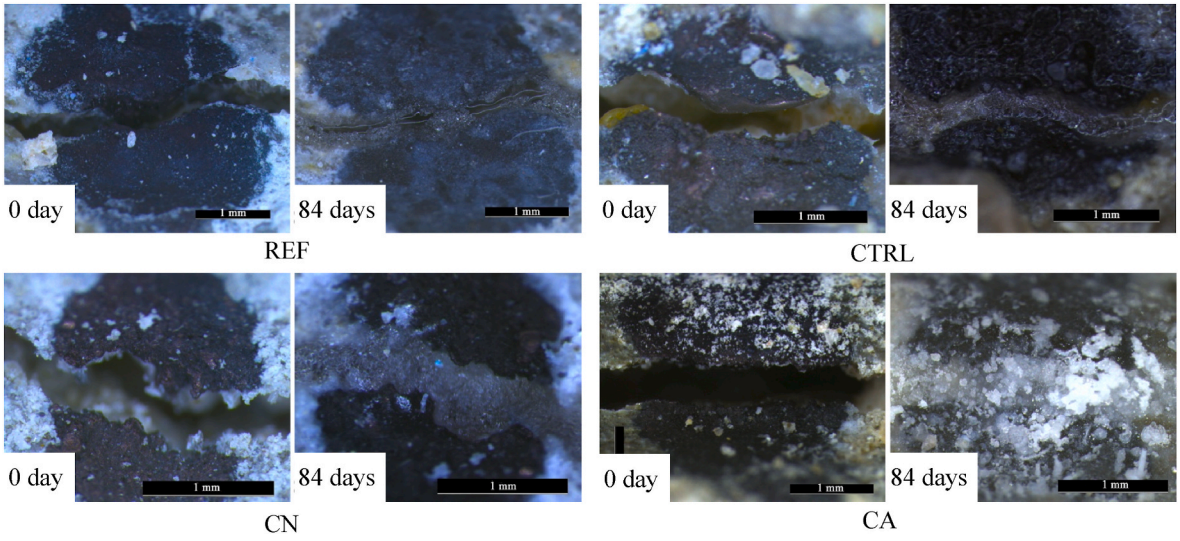

Fig. 12. Progression of crack healing of specimens in semi-submerged healing regime.

to the dissolution of calcium peroxide, raising the local calcium concentration.

4. Discussion

4.1. Healing efficiency in different healing regimes

Oxygen is not only needed for the germination of bacterial spores from aerobic species, but also for subsequent cell growth of the bacteria and the production of CO_2 from the metabolic breakdown of organic nutrients [52,59,67]. Therefore, in this research, four healing conditions with differences in availability of water and oxygen, including introducing an oxygen-releasing substance (i.e., calcium peroxide) in BBSHCC, were investigated. As per the visual crack-width observation and water-flow tests, differences in the self-healing efficiency of nominally identical BBSHCC can be observed when incubated in the four different healing regimes (See Fig. 18).

In the healing results of REF and CTRL specimens, which were principally healed via autogenous healing, CTRL performed better than REF in all healing regimes except daily wet-dry cycle DM regime, which will be discussed separately later. Autogenous healing is achieved mainly by the hydration of unhydrated cement particles and

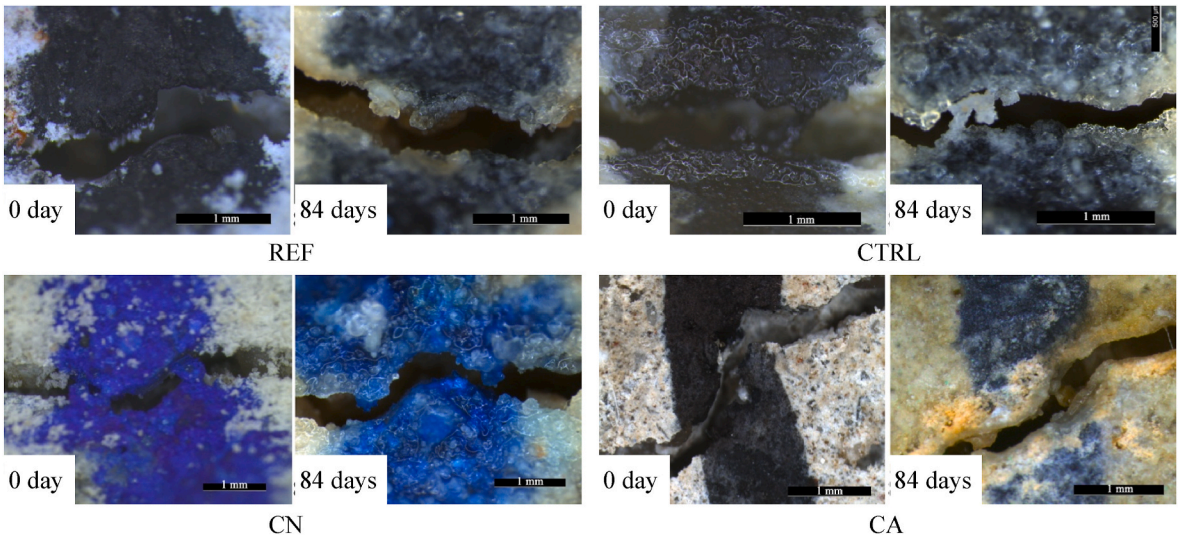

Fig. 13. Progression of crack healing of specimens in daily wet-dry cycle deposition medium healing regime.

Table 3
Mean value of initial (0 days) and final water (84 days) flow coefficient of mortar specimens.

	A. Daily wet-dry cycle			B. Weekly wet-dry cycle		
	Initial K_0	Final K_1	R_P%	Initial K_0	Final K_1	R_P%
REF	0.056	0.035	35%	0.078	0.074	5%
CTRL	0.075	0.0006	99%	0.080	0.022	72%
CN	0.045	0.0002	99%	0.010	0.050	50%
CA	0.063	0.0001	100%	0.090	0.070	22%
CNO	0.014	0.00002	99%	0.066	0.025	62%
CAO	0.032	0.00001	100%	0.066	0.020	69%
	C. Semi-submerged			**D. Deposition medium**		
	Initial K_0	Final K_1	R_P%	Initial K_0	Final K_1	R_P%
REF	0.087	0.028	67%	0.154	0.052	66%
CTRL	0.080	0.001	99%	0.216	0.074	66%
CN	0.086	0.000	100%	0.060	0.026	57%
CA	0.133	0.002	99%	0.030	0.015	50%

precipitation of calcium carbonate [34]. The healing values for REF specimens were significant higher when incubated in semi-submerged conditions (R_W: 47%; R_P: 67%) than in the daily and weekly wet-dry healing regimes (daily: R_W: 0%; R_P: 35%; weekly: R_W: 2%; R_P: 5%). The enhanced healing observed in semi-submerged REF specimens may be due to the mobilisation of calcium hydroxide from the supersaturated pore solution within the cement matrix to the water continuously present in the edges of the crack [68]. The permanent thin layer of water present within the crack likely allows the concentration of calcium to build up over time and reach a supersaturation condition, which, when exposed to a continuous source of atmospheric CO_2, could lead to the precipitation of calcium carbonates. In contrast, when REF specimens were exposed to wet-dry cycles, either daily or weekly, the water available within the cracks was part of the total volume of healing water, not allowing a build up of calcium ions at the edges of the crack.

On the other hand, the enhanced healing in CTRL over REF may be due to the conversion of calcium nitrate to calcium hydroxide and its mobilisation to the crack area, permitting more autogenous carbonation-based healing. Moreover, the presence of yeast extract within the mortar matrix likely contributed to this, as certain organic compounds are known to increase the solubility of calcium hydroxide considerably [69]. Alternatively, as tap water was used for the healing water and a carbon source (i.e., yeast extract) was readily available, it is possible that some environmental bacteria present in this water were capable of thriving in the conditions, and in the presence of abundant calcium ions, induced the precipitation of some, albeit limited, calcium carbonate. Overall, the CTRL samples performed better in daily wet-dry and semi-submerged healing regimes suggesting that the autogenous healing observed depended on the presence of water, possibly to aid in the dissolution and mobilisation of the growth media.

In general, the continuous presence of water was shown to be essential to the healing of BBSHCC (Fig. 18). Mortars containing self-healing components (CN, CA, CNO and CAO) led to almost complete crack closure (R_W: 94–100%) and recovery of water-flow resistance (R_P:99–100%) when exposed to the most water-abundant conditions (daily wet-dry cycle and semi-submerged regimes), but not in the conditions where water was unavailable for an extended time (weekly wet-dry cycle regime) and thus, where the specimens were able to completely dry (R_W: 0–50%; R_P: 22–69%). Comparing the healing results of CN and CA specimens when water was readily available (daily wet-dry cycle and semi-submerged) and when water was more limited allowing the specimens to dry for an extended period (weekly wet-dry cycle), CN illustrated higher R_W and R_P values than CA. Given that the growth media in CA were encapsulated, as opposed to the direct addition in CN, it is hypothesised that the increased requirement for water to heal cracks in CA specimens was due to the need to release the growth media from the ACGM particles.

When additional growth media was added in the healing water (daily wet-dry cycle DM regime), REF and CTRL specimens showed only large cubic crystals attached to the mouths of the cracks instead of dense precipitates. Even so, REF had rather high healing values (R_W: 50%; R_P: 66%) when compared to the other three healing regimes, suggesting that the additional calcium ions potentially combined with alkalis present in the mortar matrix to form calcium hydroxide, which was consequently carbonated to calcite. When compared to REF, the R_W observed for CTRL was 36% lower, while the R_P was the same (R_P:66%). However, as R_W healing values reflects only the healing obtained in three specific locations as opposed to R_P healing values which are obtained evaluating the complete crack, it is considered that the R_P better reflects the performance of REF and CTRL specimens. The very similar healing of REF and CTRL in this healing regime is likely attributed to the extra calcium ions provided by the DM. Nevertheless, when comparing the healing values of CTRL specimens exposed to the two healing regimes which only differ in the addition, or not, of additional growth media to the healing water (i.e., daily wet-dry cycle and daily wet-dry cycle DM), a clear difference in the healing performance was observed. The CTRL specimens exposed to the DM presented significantly lower R_W and R_P healing values (60% and 33%, respectively) than the CTRL specimens exposed to tap water. Correlating to the mixing proportion, we suggest that the intrinsically embedded calcium nitrate in the matrix of CTRL caused the

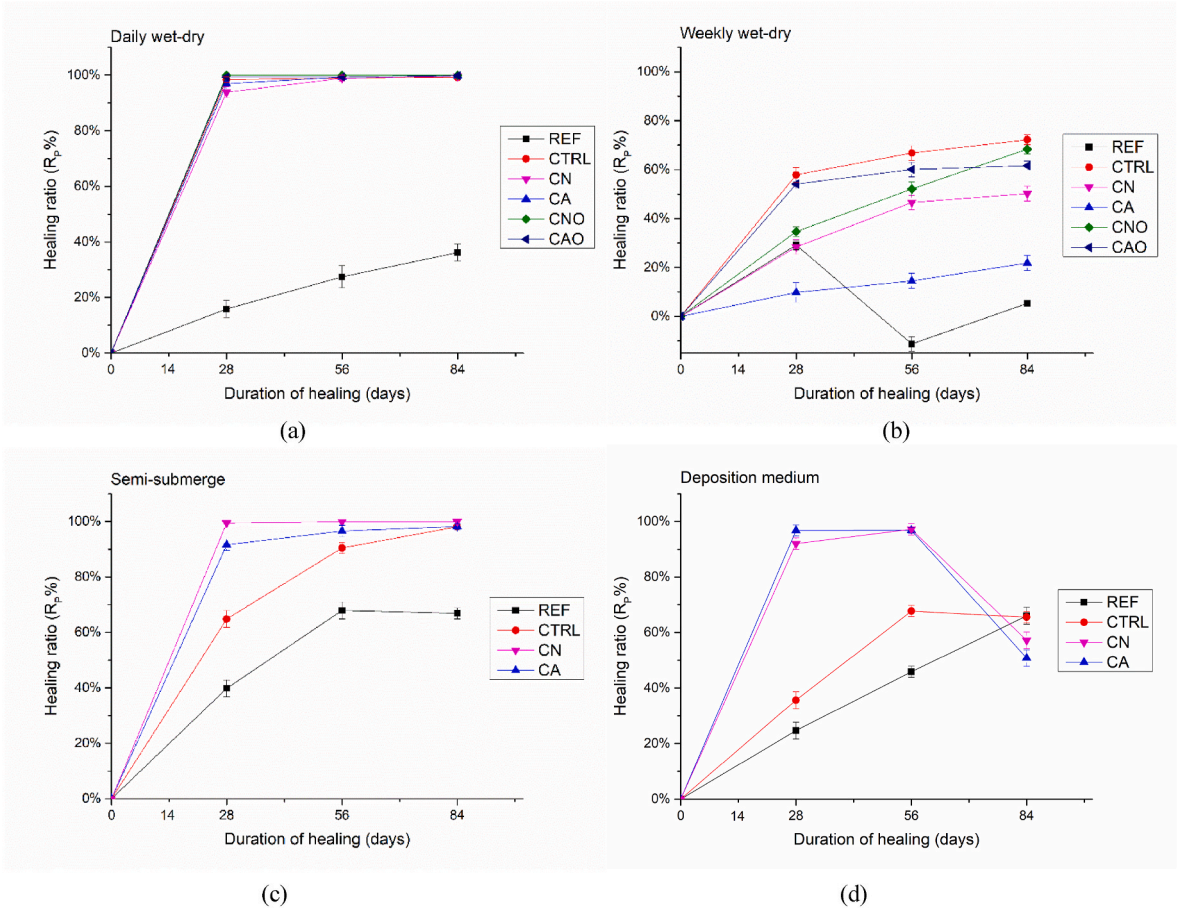

Fig. 14. Water-flow test results of R_P values over the progress of samples in (a) daily wet-dry healing regime, (b) weekly wet-dry healing regime, (c) semi-submerged healing regime and (d) daily wet-dry deposition medium healing regime.

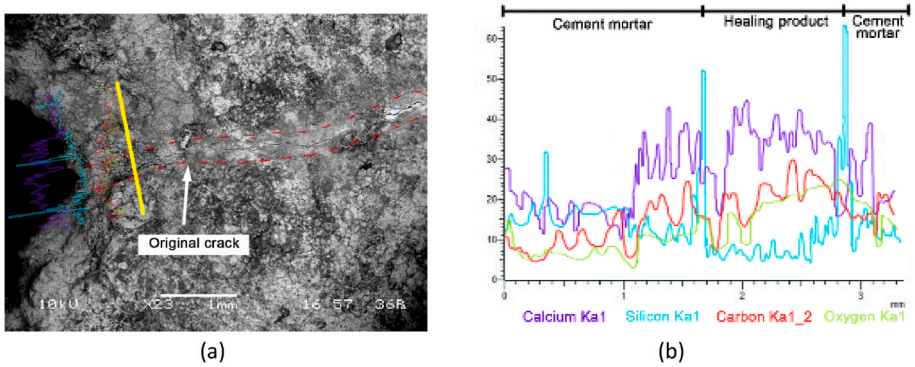

Fig. 15. (a) SEM image of a CN mortar prism (exposed for 84 days to a semi-submerged healing regime) at the crack mouth location, (b) SEM-EDX line scan elemental analysis through the self-healing product (drawn line). The line was drawn close to the mouth of the crack, and the concentration of Ca, Si, C and O is shown in (b) where the healing products' area is highlighted.

oversaturation of calcium hydroxide in the vicinity of crack, preventing the conversion of calcium hydroxide into calcium carbonate [34].

Similarly, when bacteria-based mortars (CN and CA) were exposed to the DM healing regime, significantly lower healing values were observed when compared to an equivalent healing regime (i.e., daily wet-dry cycle regime) (Fig. 18). To provide extra calcium source and nutrients for bacteria, 2 g/l yeast extract and 10 g/l calcium (either as calcium acetate or calcium nitrate) were added to the healing water in the daily wet-dry cycle DM system. During the first 56 days of healing, crack-width visual observations and water flow coefficients showed, in general, a more rapid healing compared with equivalent mortars exposed to the other three healing regimes (Figs. 9 and 14). However, the formed precipitates disappeared quickly in the following 28 days (between 56-day and 84-day), resulting in a reopened crack. The following hypotheses are suggested to explain the dissolution of precipitates observed at 84 days. The additional calcium and nutrients (i.e., yeast extract) in the DM allowed the purposely added bacteria to successfully grow and thrive during the first 56 days of incubation. In this regard, Zhang et al. [70] observed that when the yeast extract concentration was increased up to 5 g/l in bacterial sporulation medium, the amount of bacterial spore viability and calcium precipitation increased remarkably. However, once the crack was sealed with the formed precipitates, these

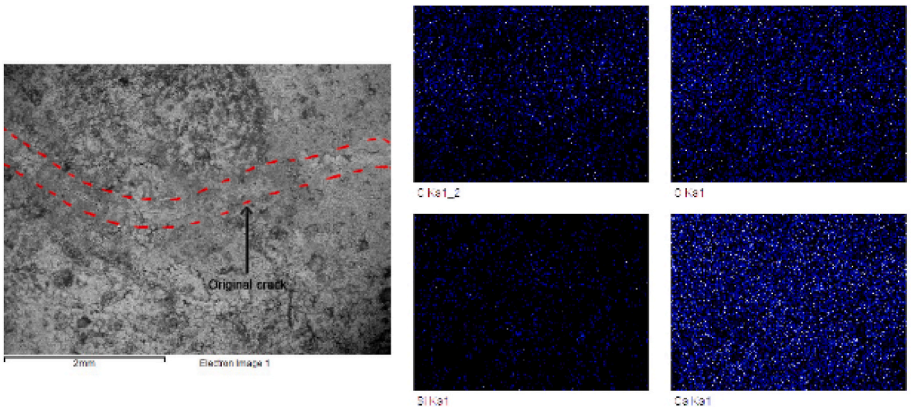

Fig. 16. SEM image of a CN healed crack after exposure to a daily wet-dry cycle healing regime (84 days) and EDX elemental maps showing: (a) carbon, (b) oxygen, (c) silicon and (d) calcium. The edges of the original crack are marked with red dotted lines. (For interpretation of the references to colour in this figure legend, the reader is referred to the Web version of this article.)

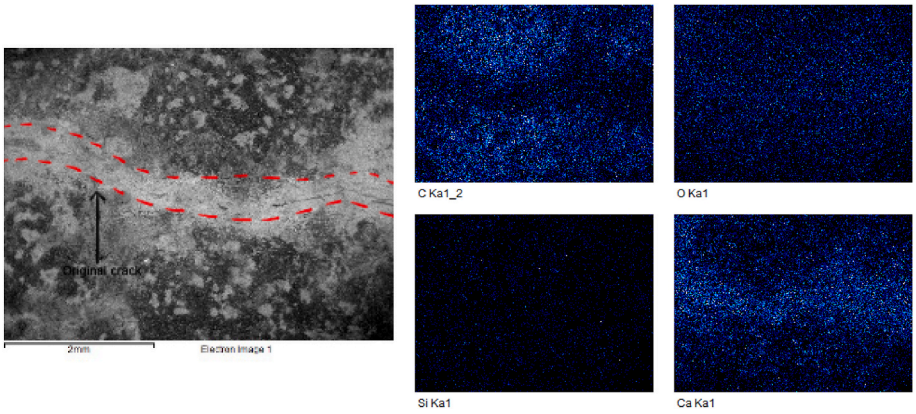

Fig. 17. Overview picture of a CNO healed crack after exposure to a daily wet-dry cycle healing regime (84 days) and EDX elemental maps showing: (a) carbon, (b) oxygen, (c) silicon and (d) calcium. The edges of the original crack are marked with red dotted lines. (For interpretation of the references to colour in this figure legend, the reader is referred to the Web version of this article.)

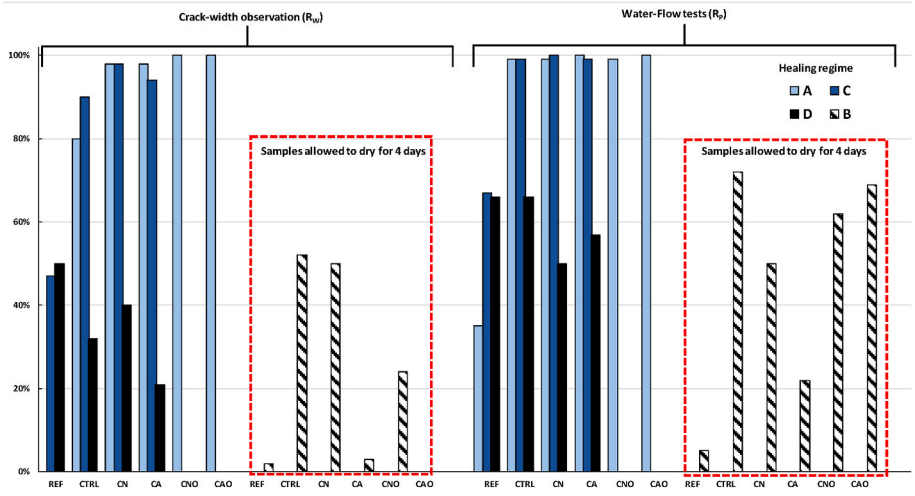

Fig. 18. Summary of the mean healing values obtained of the five mortar mixes (REF, CTRL, CN, CA, CNO and CAO) incubated in four different healing regimes (daily wet-dry cycle (A), weekly wet-dry cycle (B), semi-submerged (C) and daily wet-dry cycle deposition medium (D)) obtained from: Left: visual crack-width observation (R_W) and right: water-flow tests (R_P). The healing values for the weekly wet-dry healing regime (B) (no continuous water supply) are shown framed by a red dotted line. (For interpretation of the references to colour in this figure legend, the reader is referred to the Web version of this article.)

bacteria likely perished due to changes in the environment within the crack (e.g., less oxygen available, calcium concentration toxic the bacteria, pH changes, etc.), and thus, calcite production was halted. After 56 days of healing and with no bacteria remaining to induce calcium precipitation, the precipitates were gradually dissolved. Yeast extract as the water-soluble portion of autolysed yeast (i.e., self-digested using their own enzymes) is an organic compound with a very high protein content (~74%) [71]. In this context, it is known that certain organic compounds can increase the solubility of calcium ions [69]. Therefore, the presence of yeast extract in the DM solution could have likely resulted in the leaching of calcium ions from the precipitates with their consequent dissolution; particularly if rather than calcite, a less stable polymorph of

calcium carbonate has formed in this environment. Moreover, as no viable bacteria were remaining within the crack after 56 days to induce calcite precipitation and due to the lower pH value of the DM solution when compared to tap water [34], additional leaching of calcium from the precipitates could potentially have occurred.

In summary, mortars presented different degrees of healing depending on the healing regime they were exposed to. In general, healing regimes where tap water was readily available (daily wet-dry cycle and semi-submerged regimes) were the most effective, both for autogenous and autonomous healing. In contrast, when specimens were allowed to dry for four days (weekly wet-dry cycle regime) or alternatively submerged in a calcium/yeast extract concentrated solution (daily wet-dry cycle DM regime), the healing performance was compromised. Regarding the DM regime, the additional supply of calcium and yeast extract promoted healing at the early stage of the bacteria-based mortars (i.e., CN and CA). However, with the death of bacteria at the later stage, calcite production stopped in parallel with exposure of the specimens to a more acidic healing water containing relatively high concentrations of yeast extract, which eventually resulted in the dissolution of the precipitates within the crack.

4.2. Effect of oxygen-releasing coating (ORC) on the healing performance

SEM images of ORC-ACGS (Fig. 8 (c)) evidenced that these particles had been successfully coated with the ORC containing PVA, calcium peroxide and a water-resistant adhesive, thus, confirming the feasibility of using ORC on ACGS. Furthermore, the calculation of the coating thickness suggested a negligible influence of introducing ORC on the morphology and size of these coated ORC-ACG particles.

The kinetics of cement hydration, as shown in Fig. 6, suggested that PVA and ORC coatings effectively prevented a rupture of ACG particles during the mixing process, as no hydration delay was observed for either CA or CAO mixes, where PVA- and ORC-coated ACG particles were both added without any direct addition of growth media to mixing water. On the other hand, CN and CNO both presented an almost identical hydration delay (i.e., 8 h) when compared to REF, which can be likely attributed to the direct addition of growth media to the mixing water and not due to the influence of PVA- or OCR-coated ACG particles. Furthermore, total heat generated after 72 h was similar for all mortar mixes.

Mortar prims containing ORC-ACGS (CNO and CAO) were only exposed to daily and weekly wet-dry cycle regimes (Fig. 18). After being exposed to the daily wet-dry cycle regime, both CNO and CAO presented complete crack closure (R_W:100%; R_P:99–100%), with a slightly improved or equal healing performance when compared to CN and CA (R_W:98%; R_P:99–100%). The increased healing capacity observed for CNO and CAO suggests that the introduction of ORC benefits healing performance. On the other hand, when exposed to the weekly wet-dry healing regime, the healing values in CNO and CAO were lower than in the daily wet-dry cycle regime, consistent with the need for frequent water provision discussed above. Interestingly, although CAO and CNO showed lower R_W values than CA and CN, the R_p values of CAO and CNO were higher than the observed for CA and CN, respectively. This may have been because more healing occurred deep in the crack of CNO and CAO, possibly due to the oxygen supplement derived from ORC deep within crack.

While oxygen is the main product resulting from the reaction of the oxygen-releasing material (calcium peroxide) with water, calcium hydroxide is also formed as a by-product of the dissolution of calcium peroxide. It has been argued that additional calcium sources in BBSHCCs are sufficient to react with CO_3^{2-} to form enough calcite to seal the crack [72]. From the elementary map of CNO mortar given in Fig. 17, the calcium concentration was noticeably higher in the crack area than in the mortar matrix. In contrast, in a similar area of the CN mortar, calcium was uniformly distributed, confirming that CAO had more calcium-based precipitates formed within crack. Therefore, it is plausible to consider that these calcium-based crystals were derived from enhanced MICP due to the additional oxygen and calcium released from ORC-ACGS particles.

Derived from the results, it can be concluded that relying on a weekly wet-dry cycle healing regime to deliver more oxygen to the mortar by shortening the wetting period did not seem to achieve efficient healing. Therefore, the findings of this study evidence the importance of providing more accessible oxygen to bacteria directly inside the cracks. Moreover, the indication that ORC provided more calcium to the mortar further proved the feasibility of using ORC in BBSHCCs. In summary, providing water and oxygen simultaneously, along with an additional calcium supply, can be seen as an alternative method to improve the effectiveness of BBSHCCs.

4.3. Comparison between the utilisation of calcium nitrate and calcium acetate as calcium source

Calcium nitrate and calcium acetate were used in this study as a calcium source for MICP, although the way in which they were included differed. Whilst an investigation of the calcium carbonate precipitating ability with use of different calcium sources was not a primary objective of this research, for the sake of completeness, a discussion is presented here of the differences in healing performance observed when either calcium nitrate or calcium acetate were used.

From the visual crack-width observations and water-flow coefficient results when using tap water (i.e., not DM), calcium nitrate-based specimens showed generally greater healing in the weekly wet-dry cycle and semi-submerged regimes than calcium acetate-based mortars. In contrast, mortars exposed to the daily wet-dry cycle regime presented similar healing values (i.e., 98%–100%). It should be remembered that both calcium precursors were added to the mortars in different ways. Calcium nitrate and yeast extract were directly added to the mortar during mixing, whilst calcium acetate and yeast extract were encapsulated into ACGM particles. Considering the different operating mechanism of each healing regime, calcium acetate-based mortar illustrated more remarkable healing in conditions where the specimens were regularly completely saturated (daily wet/dry cycle), whereas calcium nitrate-based mortar could still produce a considerable amount of calcite in an environment with less water availability (weekly wet-dry cycle). In this regard, considering the growth media was encapsulated for CA and CAO specimens, it may be possible that the regular complete submersion could help with the release of nutrients/calcium from the ACG particles and their consequent diffusion *via* the water to the bacteria active within the crack.

Since carbon is missing in calcium nitrate ($Ca(NO_3)_2$), DIC needs to be supplied from elsewhere to obtain calcite ($CaCO_3$). In the mortars used in this research this is partially accomplished by the provision of yeast extract for bacterial metabolism. Moreover, from the results obtained, calcium nitrate-based mortars, including CNO, appeared to perform better in regimes with an extended dry phase, in comparison with calcium acetate-based mortars, providing an opportunity for external CO_2 to absorb into the mortar, providing further DIC to be used in MICP during the next wet phase. Thus, under conditions where yeast extract is provided as the only carbon source to the bacteria (i.e., without additional acetate), the extended access to air from weekly wet-dry cycling or semi-submerged incubation may be beneficial to calcite formation. In contrast, samples containing both acetate and yeast extract to provide the DIC mostly benefited from the regular presence of water in the daily wet-dry cycle.

Overall, it can be concluded that the direct addition of bio-agents makes calcium source and yeast extract more accessible to bacteria. However, such a provision necessitates the use of calcium nitrate as opposed to calcium acetate to compensate for the retardation of cement caused by direct addition of yeast extract. Thus, despite the reduced provision of organic sources for DIC when calcium nitrate is used, it can be argued that calcium nitrate is an overall better calcium source for

MICP when yeast extract or other carbon sources are adequately available.

5. Conclusions

Availability of water and oxygen has been shown to be essential to successful bacteria-based self-healing of cementitious composites. Importantly, it has been observed that drying of composites, for even a short time, significantly affects the healing performance. This has important consequences for the development of appropriate test standards for self-healing cementitious composites, and for the design and implementation of such cementitious composites in practice.

Furthermore, calcium peroxide was shown to be successfully coated onto aerated concrete granules (ACG) and able to release additional oxygen and calcium during the healing process, which resulted in the enhanced healing efficiency observed in ORC-containing BBSHCCs. Therefore, the following specific conclusions can be drawn:

1. Compared with calcium nitrate-based specimens, calcium acetate-based specimens required more water, likely to successfully release and disperse encapsulated nutrients. Calcium nitrate-based specimens generally showed the greatest healing performance when more DIC was available.
2. Oxygen-releasing coating (ORC) was confirmed to remained intact and unreacted during the mixing process and to have minor effects on the physical properties and morphology of OCR-coated ACG particles.
3. In general, healing was most pronounced in conditions where both water and oxygen were regularly available to the bacteria. Conversely, conditions where oxygen or water were not readily available for extended periods (weekly wet-dry regime) resulted in significantly less effective healing, especially for BBSHCCs not containing OCR-ACGS.
4. An overdose of nutrients and calcium ions in the healing environment may induce rapid precipitation at an early stage. However, with the death of bacteria at a later stage, the high concentrations of yeast extract and calcium ions present in the water within the crack may lead to the dissolution of the precipitates and, consequently, lower quality of healing.
5. The use of ORC-coated particles to provide an additional supply of oxygen and calcium can be seen as an alternative method to improve the effectiveness of BBSHCCs, especially the promotion of healing deep within cracks.

Declaration of competing interest

The authors declare the following financial interests/personal relationships which may be considered as potential competing interests: Kevin Paine reports financial support was provided by Engineering and Physical Sciences Research Council.

Data availability

Data will be made available on request.

Acknowledgements

The authors acknowledge the Engineering and Physical Sciences Research Council (Grant No. EP/P02081X/1) and Industrial collaborators/partners for funding the Resilient Materials for Life (RM4L) project. The authors gratefully acknowledge the technical staff in the Department of Architecture and Civil Engineering, the Department of Biology and Biochemistry and the Material and Chemical Characterisation Facility (MC^2) at the University of Bath (https://doi.org/10.15125/mx6j-3r54) for their key support.

References

[1] V.G. Papadakis, M.N. Fardis, C.G. Vayenas, Effect of composition, environmental factors and cement-lime mortar coating on concrete carbonation, Mater. Struct. 25 (1992) 293–304.
[2] Office for National Statistics, Infrastructure in the UK, Investment and Net Stocks: May 2022, Office for National Statistics, UK, 2022. Statistics report 18 May 2022 2022.
[3] A. Beglarigale, D. Eyice, B. Tutkun, H. Yazici, Evaluation of enhanced autogenous self-healing ability of UHPC mixtures, Construct. Build. Mater. 280 (2021), 122524.
[4] K. Tomczak, J. Jakubowski, Ł. Kotwica, Enhanced autogenous self-healing of cement-based composites with mechanically activated fluidized-bed combustion fly ash, Construct. Build. Mater. 300 (2021), 124028.
[5] R. Maddalena, H. Taha, D. Gardner, Self-healing potential of supplementary cementitious materials in cement mortars: sorptivity and pore structure, Dev. Built Environ. 6 (2021), 100044.
[6] C. Joseph, A.D.D. Jefferson, B. Isaacs, R. Lark, D. Gardner, Experimental investigation of adhesive-based self-healing of cementitious materials, Mag. Concr. Res. 62 (2010) 831–843, https://doi.org/10.1680/macr.2010.62.11.831.
[7] V.C. Li, Y.M. Lim, Y.-W. Chan, Feasibility study of a passive smart self-healing cementitious composite, Compos. B Eng. 29 (1998) 819–827.
[8] C.M. Dry, lt;title>Design of self-growing, self-sensing, and self-repairing materials for engineering applications</title&gt, Smart Mater 4234 (2001) 23–29, https://doi.org/10.1117/12.424430.
[9] C. Joseph, A.D. Jefferson, M.B. Cantoni, Issues relating to the autonomic healing of cementitious materials, in: First Int. Conf. Self-Healing Mater., 2007, pp. 1–8.
[10] G. Perez, E. Erkizia, J.J. Gaitero, I. Kaltzakorta, I. Jiménez, A. Guerrero, Synthesis and characterization of epoxy encapsulating silica microcapsules and amine functionalized silica nanoparticles for development of an innovative self-healing concrete, Mater. Chem. Phys. 165 (2015) 39–48.
[11] T. Nishiwaki, H. Mihashi, B.K. Jang, K. Miura, Development of self-healing system for concrete with selective heating around crack, J. Adv. Concr. Technol. 4 (2006) 267–275, https://doi.org/10.3151/jact.4.267.
[12] T.D.P. Thao, T.J.S. Johnson, Q.S. Tong, P.S. Dai, Implementation of self-healing in concrete–proof of concept, IES J. Part A Civ. Struct. Eng. 2 (2009) 116–125.
[13] W. Mao, C. Litina, A. Al-Tabbaa, Development and application of novel sodium silicate microcapsule-based self-healing oil well cement, Materials (Basel) 13 (2020) 456.
[14] C. Litina, A. Al-Tabbaa, First generation microcapsule-based self-healing cementitious construction repair materials, Construct. Build. Mater. 255 (2020), 119389.
[15] T.A. de Oliveira, M.D.G.P. Bragança, I.M. Pinkoski, G. Carrera, The effect of silica nanocapsules on self-healing concrete, Construct. Build. Mater. 300 (2021), 124010.
[16] N.P.B. Tan, L.H. Keung, W.H. Choi, W.C. Lam, H.N. Leung, Silica-based self-healing microcapsules for self-repair in concrete, J. Appl. Polym. Sci. 133 (2016).
[17] C.M. Dry, Design of self-growing, self-sensing, and self-repairing materials for engineering applications, in: Smart Mater., International Society for Optics and Photonics, 2001, pp. 23–29.
[18] H. Mihashi, Y. Kaneko, T. Nishiwaki, K. Otsuka, Fundamental study on development of intelligent concrete characterized by self-healing capability for strength, Trans. Japan Concr. Inst. 22 (2001) 441–450.
[19] I. Justo-Reinoso, A. Heath, S. Gebhard, K. Paine, Aerobic non-ureolytic bacteria-based self-healing cementitious composites: a comprehensive review, J. Build. Eng. 42 (2021), 102834, https://doi.org/10.1016/j.jobe.2021.102834.
[20] S. Indhumathi, A. Dinesh, M. Pichumani, Diverse perspectives on self healing ability of Engineered Cement Composite–All-inclusive insight, Construct. Build. Mater. 323 (2022), 126473.
[21] H. Kim, H.M. Son, J. Seo, H.K. Lee, Recent advances in microbial viability and self-healing performance in bacterial-based cementitious materials: a review, Construct. Build. Mater. 274 (2021), 122094, https://doi.org/10.1016/j.conbuildmat.2020.122094.
[22] T.H. Nguyen, E. Ghorbel, H. Fares, A. Cousture, Bacterial self-healing of concrete and durability assessment, Cem. Concr. Compos. 104 (2019), 103340.
[23] W. De Muynck, N. De Belie, W. Verstraete, Microbial carbonate precipitation in construction materials: a review, Ecol. Eng. 36 (2010) 118–136, https://doi.org/10.1016/j.ecoleng.2009.02.006.
[24] K. Van Tittelboom, N. De Belie, Self-healing in cementitious materials—a review, Materials (Basel) 6 (2013) 2182–2217.
[25] M. Wu, B. Johannesson, M. Geiker, A review: self-healing in cementitious materials and engineered cementitious composite as a self-healing material, Construct. Build. Mater. 28 (2012) 571–583, https://doi.org/10.1016/j.conbuildmat.2011.08.086.
[26] N. De Belie, E. Gruyaert, A. Al-Tabbaa, P. Antonaci, C. Baera, D. Bajare, A. Darquennes, R. Davies, L. Ferrara, T. Jefferson, C. Litina, B. Miljevic, A. Otlewska, J. Ranogajec, M. Roig-Flores, K. Paine, P. Lukowski, P. Serna, J. M. Tulliani, S. Vucetic, J. Wang, H.M. Jonkers, A review of self-healing concrete for damage management of structures, Adv. Mater. Interfac. 5 (2018) 1–28, https://doi.org/10.1002/admi.201800074.
[27] D. Palin, V. Wiktor, H.M. Jonkers, Abacteria-based bead for possible self-healing marine concrete applications, Smart Mater. Struct. 25 (2016), 84008, https://doi.org/10.1088/0964-1726/25/8/084008.
[28] K. Paine, I. Horne, L. Tan, T. Sharma, A. Heath, R. Cooper, J. Virgoe, D. Palmer, A. Kerr, Microencapsulated spores and growth media for self-healing mortars, in: Taerwe Caspeele, Frangopol (Eds.), Life-Cycle Anal. Assess. Civ. Eng. Towar. An Integr. Vis., Taylor & Francis Group, 2019, pp. 2247–2253.

[29] M.F. A, H. M, L. Dufossé, Microbial calcite induction : a magic that fortifies and heals concrete, Int. J. Environ. Sci. Technol. (2022), https://doi.org/10.1007/s13762-022-03941-2.
[30] R. Garg, R. Garg, N.O. Eddy, Microbial induced calcite precipitation for self-healing of concrete: a review, J. Sustain. Cem. Mater. (2022) 1–14.
[31] W. De Muynck, K. Cox, N. De Belie, W. Verstraete, Bacterial carbonate precipitation as an alternative surface treatment for concrete, Construct. Build. Mater. 22 (2008) 875–885, https://doi.org/10.1016/j.conbuildmat.2006.12.011.
[32] S.K. Ramachandran, V. Ramakrishnan, S.S. Bang, Remediation of concrete using micro-organisms, ACI Mater. J. 98 (2001) 3–9, https://doi.org/10.14359/10154.
[33] K. Sarayu, N.R. Iyer, A.R. Murthy, Exploration on the biotechnological aspect of the ureolytic bacteria for the production of the cementitious materials—a review, Appl. Biochem. Biotechnol. 172 (2014) 2308–2323.
[34] J.Y. Wang, H. Soens, W. Verstraete, N. De Belie, Self-healing concrete by use of microencapsulated bacterial spores, Cem, Concr. Res. 56 (2014) 139–152, https://doi.org/10.1016/j.cemconres.2013.11.009.
[35] N. De Belie, J. Wang, Z.B. Bundur, K. Paine, Bacteria-based concrete, in: Eco-Efficient Repair Rehabil. Concr. Infrastructures, Woodhead Publishing, 2018, pp. 531–567, https://doi.org/10.1007/978-1-4939-6881-7.
[36] W. Zhang, Q. Zheng, A. Ashour, B. Han, Self-healing cement concrete composites for resilient infrastructures: a review, Compos. B Eng. 189 (2020), 107892.
[37] W. Zhang, D. Wang, B. Han, Self-healing concrete-based composites, in: Self-Healing Compos. Mater., Elsevier, 2020, pp. 259–284.
[38] M. Zamani, S. Nikafshar, A. Mousa, A. Behnia, Bacteria encapsulation using synthesized polyurea for self-healing of cement paste, Construct. Build. Mater. 249 (2020), 118556.
[39] A.M. Neville, J.J. Brooks, Concrete Technology, Longman Scientific & Technical England, 1987.
[40] H.M. Jonkers, A. Thijssen, G. Muyzer, O. Copuroglu, E. Schlangen, H.M. Jonkers, A. Thijssen, G. Muyzer, O. Copuroglu, E. Schlangen, Application of bacteria as self-healing agent for the development of sustainable concrete, Ecol. Eng. 36 (2010) 230–235, https://doi.org/10.1016/j.ecoleng.2008.12.036.
[41] H.M. Jonkers, E. Schlangen, Self-healing of cracked concrete: a bacterial approach, Proc. FRACOS6 Fract. Mech. Concr. Concr. Struct. Catania, Italy. (2007) 1821–1826.
[42] M.S.A. Alazhari, Effect of Microbiological Agents on the Efficiency of Bio-Based Repair Systems for Concrete, PhD thesis, University of Bath, 2017.
[43] L. Tan, B. Reeksting, V. Ferrandiz-Mas, A. Heath, S. Gebhard, K. Paine, Effect of carbonation on bacteria-based self-healing of cementitious composites, Construct. Build. Mater. 257 (2020), 119501, https://doi.org/10.1016/j.conbuildmat.2020.119501.
[44] L. Tan, X. Ke, Q. Li, S. Gebhard, V. Ferrandiz-Mas, K. Paine, W. Chen, The effects of biomineralization on the localised phase and microstructure evolutions of bacteria-based self-healing cementitious composites, Cem. Concr. Compos. 128 (2022), 104421, https://doi.org/10.1016/j.cemconcomp.2022.104421.
[45] T.D. Brock, M.T. Madigan, J.M. Martinko, J. Parker, Brock Biology of Microorganisms, Prentice-Hall, Upper Saddle River (NJ), 2003, p. 2003.
[46] B.M. Mortensen, M.J. Haber, J.T. DeJong, L.F. Caslake, D.C. Nelson, Effects of environmental factors on microbial induced calcium carbonate precipitation, J. Appl. Microbiol. 111 (2011) 338–349.
[47] M.N. Uddin, T. Tafsirojjaman, N. Shanmugasundaram, S. Praveenkumar, L. Li, Smart self-healing bacterial concrete for sustainable goal, Innov. Infrastruct. Solut. 8 (2023) 46.
[48] C. Rodriguez-Navarro, M. Rodriguez-Gallego, K. Ben Chekroun, M.T. Gonzalez-Munoz, Conservation of ornamental stone by Myxococcus xanthus-induced carbonate biomineralization, Appl. Environ. Microbiol. 69 (2003) 2182–2193.
[49] J. Wang, H.M. Jonkers, N. Boon, N. De Belie, Bacillus sphaericus LMG 22257 is physiologically suitable for self-healing concrete, Appl. Microbiol. Biotechnol. 101 (2017) 5101–5114, https://doi.org/10.1007/s00253-017-8260-2.
[50] M. Grinberg, T. Orevi, S. Steinberg, N. Kashtan, Bacterial survival in microscopic surface wetness, Elife 8 (2019), e48508.
[51] J. Wang, N. De Belie, Effect of water availability on microbial self-healing of concrete, in: 1st Concr, Innov. Conf. (CIC 2014), 2014, pp. 1–8.
[52] J. Wang, A. Mignon, D. Snoeck, V. Wiktor, S. Van Vliergerghe, N. Boon, N. De Belie, Application of modified-alginate encapsulated carbonate producing bacteria in concrete: a promising strategy for crack self-healing, Front. Microbiol. 6 (2015) 1–14, https://doi.org/10.3389/fmicb.2015.01088.
[53] V. Wiktor, H.M. Jonkers, Quantification of crack-healing in novel bacteria-based self-healing concrete, Cem. Concr. Compos. 33 (2011) 763–770, https://doi.org/10.1016/j.cemconcomp.2011.03.012.
[54] B.J. Reeksting, T.D. Hoffmann, L. Tan, K. Paine, S. Gebhard, In-depth profiling of calcite precipitation by environmental bacteria reveals fundamental mechanistic differences with relevance to application, Appl. Environ. Microbiol. 86 (2020) 1–16, https://doi.org/10.1128/aem.02739-19.
[55] M. Alazhari, T. Sharma, A. Heath, R. Cooper, K. Paine, Application of expanded perlite encapsulated bacteria and growth media for self-healing concrete, Construct. Build. Mater. 160 (2018) 610–619, https://doi.org/10.1016/j.conbuildmat.2017.11.086.
[56] E. Tziviloglou, V. Wiktor, H.M. Jonkers, E. Schlangen, Bacteria-based self-healing concrete to increase liquid tightness of cracks, Construct. Build. Mater. 122 (2016) 118–125, https://doi.org/10.1016/j.conbuildmat.2016.06.080.
[57] M. Abdulkareem, F. Ayeronfe, M.Z. Abd Majid, A.R.M. Sam, J.-H.J. Kim, Evaluation of effects of multi-varied atmospheric curing conditions on compressive strength of bacterial (bacillus subtilis) cement mortar, Construct. Build. Mater. 218 (2019) 1–7.
[58] G. Vigneswaran, K. Poonguzhali, D. Gowdhaman, A. Sumathi, A. Rajesh, Performance of bacteria-based non-encapsulated self-healing concrete, in: Recent Adv. Civ. Eng. Sel. Proc. CTCS 2021, Springer, 2022, pp. 565–581.
[59] J.L. Zhang, C.G. Wang, Q.L. Wang, J.L. Feng, W. Pan, X.C. Zheng, B. Liu, N.X. Han, F. Xing, X. Deng, A binary concrete crack self-healing system containing oxygen-releasing tablet and bacteria and its Ca2+-precipitation performance, Appl. Microbiol. Biotechnol. 100 (2016) 10295–10306, https://doi.org/10.1007/s00253-016-7741-z.
[60] J. Zhang, B. Mai, T. Cai, J. Luo, W. Wu, B. Liu, N. Han, F. Xing, X. Deng, Optimization of a binary concrete crack self-healing system containing bacteria and oxygen, Materials (Basel) 10 (2017) 116, https://doi.org/10.3390/ma10020116.
[61] M.-I. A. a. T. Division, 3M Super 77 Multipurpose Adhesive (Aerosol) Safety Data Sheet, (n.d.).
[62] J.N. Cernica, Geotechnical Engineering: Soil Mechanics, Wiley, 1995.
[63] A. Amiri, Z.B. Bundur, Use of corn-steep liquor as an alternative carbon source for biomineralization in cement-based materials and its impact on performance, Construct. Build. Mater. 165 (2018) 655–662, https://doi.org/10.1016/J.CONBUILDMAT.2018.01.070.
[64] M. Roig-Flores, F. Pirritano, P. Serna, L. Ferrara, Effect of crystalline admixtures on the self-healing capability of early-age concrete studied by means of permeability and crack closing tests, Construct. Build. Mater. 114 (2016) 447–457, https://doi.org/10.1016/j.conbuildmat.2016.03.196.
[67] M.B.E. Khan, L. Shen, D. Dias-da-Costa, Self-healing behaviour of bio-concrete in submerged and tidal marine environments, Construct. Build. Mater. 277 (2021), 122332, https://doi.org/10.1016/j.conbuildmat.2021.122332.
[68] I. Justo-Reinoso, B.J. Reeksting, C. Hamley-Bennett, A. Heath, S. Gebhard, K. Paine, Air-entraining admixtures as a protection method for bacterial spores in self-healing cementitious composites : healing evaluation of early and later-age cracks, Construct. Build. Mater. 327 (2022), 126877, https://doi.org/10.1016/j.conbuildmat.2022.126877.
[69] H.H. Bache, G.M. Idorn, P. Nepper-Christensen, J. Nielsen, Morphology of calcium hydroxide in cement paste, HRB Spec. Rep. 90 (1966) 154–174.
[70] J. Zhang, Y. Liu, T. Feng, M. Zhou, L. Zhao, A. Zhou, Z. Li, Immobilizing bacteria in expanded perlite for the crack self-healing in concrete, Construct. Build. Mater. 148 (2017) 610–617, https://doi.org/10.1016/j.conbuildmat.2017.05.021.
[71] NEOGEN, Technical Specification Sheet - Yeast Extract (NCM0218), NEOGEN Culture Media, Lansing, MI (USA), 2019.
[72] J.L. Zhang, R.S. Wu, Y.M. Li, J.Y. Zhong, X. Deng, B. Liu, N.X. Han, F. Xing, Screening of bacteria for self-healing of concrete cracks and optimization of the microbial calcium precipitation process, Appl. Microbiol. Biotechnol. 100 (2016) 6661–6670, https://doi.org/10.1007/s00253-016-7382-2.